NEURODEGENERATION

Systematic analysis of cellular cross-talk reveals a role for SEMA6D-TREM2 regulating microglial function in Alzheimer's disease

Ricardo D'Oliveira Albanus[1,2,3]†, Gina M. Finan[4,5]†, Logan Brase[1,3], Nicholas Sweeney[6], Tae Yeon Kim[6], Shuo Chen[6], Yeonsu Ryoo[7,8,9], Joseph Park[7,8], Qi Guo[10], Abhirami Kannan[1,3], Mariana Acquarone[1,3], Shih-Feng You[1,3], Brenna C. Novotny[1,3], Emily M. Mace[11], Patricia M. Ribeiro Pereira[12], John C. Morris[2,3,13,14], David M. Holtzman[2,3,13,14], Eric McDade[1,14], Martin Farlow[14,15], Jasmeer P. Chhatwal[14,16], Bruno A. Benitez[17], Laura Piccio[3,18,19], Richard J. Perrin[3,2,18], Greg T. Sutherland[20], Qin Ma[10], Celeste M. Karch[1,3,14], Doo Yeon Kim[7,8], Rudolph E. Tanzi[7,8], Hongjun Fu[6,3,14], Oscar Harari[1,3]*‡, Tae-Wan Kim[4,5]*

Cellular cross-talk, mediated by membrane receptors and their ligands, is crucial for brain homeostasis and can contribute to neurodegenerative diseases such as Alzheimer's disease (AD). To find cross-talk dysregulations involved in AD, we reconstructed cross-talk networks from single-nucleus transcriptional profiles of 67 clinically and neuropathologically well-characterized controls and AD brain donors from the Knight Alzheimer Disease Research Center and the Dominantly Inherited Alzheimer Network cohorts. We predicted a role for TREM2 and additional AD risk genes mediating neuron-microglia cross-talk in AD. We identified a gene network mediating neuron-microglia cross-talk through TREM2 and neuronal SEMA6D, which we predicted is disrupted in late AD stages. Using spatial transcriptomics on the human brain, we observed that the SEMA6D-TREM2 cross-talk gene network is activated near Aβ plaques and SEMA6D-expressing cells. Using tissue immunostaining of human brains, we found that SEMA6D colocalizes with Aβ plaques and TREM2-activated microglia. In addition, we found that plaque-proximal SEMA6D abundance decreased with the disease stage, which correlated with a reduction in microglial activation near plaques. These findings suggest that the loss of SEMA6D signaling impairs microglial activation and Aβ clearance. To validate this hypothesis, we leveraged *TREM2* knockout human induced pluripotent stem cell–derived microglia and observed that SEMA6D induces microglial activation and Aβ plaque phagocytosis in a TREM2-dependent manner. In summary, we demonstrate that characterizing cellular cross-talk networks can yield insights into AD biology, provide additional context to understand AD genetic risk, and find previously unknown therapeutic targets and pathways.

INTRODUCTION

Cross-cellular signaling (cellular cross-talk) is integral to normal brain physiology. By establishing cellular networks mediated by membrane receptors and their corresponding ligands, cells can gather information from their immediate environment and respond accordingly. Cellular cross-talk is crucial to brain homeostasis and neurodevelopment processes, such as synaptic pruning and axon guidance (*1*, *2*). However, increasing experimental and genetic evidence implicates aberrant cellular cross-talk as a contributing factor to neurodegenerative diseases, including Alzheimer's disease (AD) (*3*–*6*). From a translational perspective, cellular cross-talk is an attractive molecular target for drug development, because membrane receptors are relatively amenable to therapeutic targeting (*7*–*9*). Therefore, systematic characterization of brain cellular cross-talk interactions can help identify molecular mechanisms involved in neurodegeneration and inform therapeutic strategies.

Genome-wide association studies (GWASs) have successfully identified genetic risk loci for AD and nominated genes likely mediating these genetic signals (*10*–*13*). Further, by leveraging human tissue

[1]Department of Psychiatry, Washington University School of Medicine, St. Louis, MO 63130, USA. [2]Department of Neurology, Washington University School of Medicine, St. Louis, MO 63130, USA. [3]Hope Center for Neurological Disorders, Washington University School of Medicine, St. Louis, MO 63130, USA. [4]Department of Pathology and Cell Biology, Columbia University Irving Medical Center, New York, NY 10032, USA. [5]Taub Institute for Research on Alzheimer's Disease and the Aging Brain, Columbia University Irving Medical Center, New York, NY 10032, USA. [6]Department of Neuroscience, Ohio State University Wexner Medical Center, Columbus, OH 43210, USA. [7]Genetics and Aging Research Unit, MassGeneral Institute for Neurodegenerative Disease, Department of Neurology, Massachusetts General Hospital, Harvard Medical School, Charlestown, MA 02114, USA. [8]McCance Center for Brain Health, Massachusetts General Hospital, Boston, MA 02114, USA. [9]Department of Chemistry, Hanyang University, Seoul 04763, Republic of Korea. [10]Department of Biomedical Informatics, Ohio State Comprehensive Cancer Center, Columbus, OH 43210, USA. [11]Department of Pediatrics, Columbia University, New York, NY 10032, USA. [12]Department of Radiology, Division of Radiological Sciences, Washington University School of Medicine, St. Louis, MO 63130, USA. [13]Knight Alzheimer Disease Research Center, Washington University School of Medicine, St. Louis, MO 63130, USA. [14]Dominantly Inherited Alzheimer Network (DIAN), Washington University School of Medicine, St. Louis, MO 63130, USA. [15]Department of Neurology, Indiana University School of Medicine, Indianapolis, IN 46202, USA. [16]Department of Neurology, Massachusetts General Hospital, Harvard Medical School, Boston, MA 02114, USA. [17]Department of Neurology, Beth Israel Deaconess, Harvard Medical School, Boston, MA 02215, USA. [18]Department of Pathology and Immunology, Washington University School of Medicine, St. Louis, MO 63130, USA. [19]Brain and Mind Centre, School of Medical Sciences, University of Sydney, Camperdown, NSW 2006, Australia. [20]School of Medical Sciences and Charles Perkins Centre, Faculty of Medicine and Health, University of Sydney, Sydney, NSW 2006, Australia.
*Corresponding author. Email: oscar.harai@osumc.edu (O.H.); twk16@cumc.columbia.edu (T.-W.K.)
†These authors contributed equally to this work.
‡Present address: Division of Neurogenetics, Neurobiology of Aging and Resilience Center, Ohio State University, Columbus, OH 43210, USA.

(*14*–*17*) and experimental data from human induced pluripotent stem cell (iPSC)–derived cells (*18*), functional genomics studies have revealed that many AD risk genes are expressed by microglial cells. However, how most of these microglial AD risk genes are regulated in the contexts of normal physiology and AD pathophysiology is still unknown. As the resident immune cells of the brain, microglia are highly attuned to their surrounding environment, including signals from neighboring cells (*19*). Although previous studies have shown causal effects of disrupted cross-talk in neurodegeneration, it remains unclear how cellular cross-talk between microglia and other cell types is involved in mediating AD genetic risk. Understanding these processes requires characterizing the cross-talk networks in the brain, reconstructing the likely signaling pathways downstream of these interactions, and integrating these data with genetic findings.

In this study, we reanalyzed brain single-nucleus RNA sequencing (snRNA-seq) profiles from Knight Alzheimer Disease Research Center (Knight ADRC) and Dominantly Inherited Alzheimer Network (DIAN) cohorts to systematically reconstruct the cellular cross-talk networks across seven major brain cell types. We found that the direct involvement of known AD risk genes was more frequent in neuron-microglia cross-talk interactions and identified a subnetwork of microglial genes centered around *TREM2* that we predicted mediates neuron-microglia cross-talk. We predicted that this subnetwork is modulated by the cross-talk interaction between semaphorin 6D (SEMA6D) and microglial triggering receptor expressed on myeloid cells 2 (TREM2). Using spatial transcriptomics and multiplex immunofluorescence on human brains, we found evidence that this subnetwork is disrupted in late-stage AD and activated near amyloid-β (Aβ) plaques and SEMA6D-expressing cells. We further validated our predictions in vitro using wild-type (WT) and *TREM2* knockout (KO) human iPSC-derived microglia (iMGL). Our findings suggest a complex interplay of SEMA6D signaling from multiple cell types, of which we hypothesize neurons as the predominant source, converging on the microglial TREM2 pathway to modulate AD pathophysiology.

RESULTS

A complex landscape of cross-talk dysregulation in AD

To systematically characterize cellular cross-talk interactions in controls and AD, we analyzed snRNA-seq profiles of superior parietal cortex tissue samples from 67 brain donors of the Knight ADRC and the DIAN, previously published by our group (*14*). This dataset encompasses different AD subtypes, including sporadic AD and autosomal dominant AD (ADAD), with donors distributed in a broad spectrum of neuropathological states and genetic backgrounds, including carriers of *TREM2* risk variants (table S1). In total, we analyzed approximately 300,000 nuclei representing seven major brain cell types [microglia, astrocytes, oligodendrocytes, oligodendrocyte precursors (OPCs), excitatory and inhibitory neurons, and endothelial cells] from 67 donors (Fig. 1A). We identified patterns of ligand-receptor gene expression across cell type pairs using CellPhoneDB (*20*), which has been successfully used to predict patterns of brain cellular cross-talk (*5*).

We predicted cross-talk interactions separately for disease status and genetic group in our CellPhoneDB analyses. In total, we identified between 961 and 1600 (median = 1521) significant (Bonferroni-corrected $P < 0.05$) cross-talk interactions between cell type pairs across all donor categories (Fig. 1B, fig. S1A, and table S2). We compared the cross-talk patterns across cases and controls to identify global changes associated with disease status. Globally, we predicted significantly more cross-talk interactions involving microglia in AD donors than controls (odds ratio = 1.12, $P = 0.019$, Fisher's exact test; Fig. 1B and fig. S1B). Because there is limited evidence on whether microglial numbers change during AD (*21*) and we did not observe alterations in the count of microglial nuclei associated with the disease state, we hypothesize that the increased number of predicted cross-talk interactions involving microglia in AD donors indicates transcriptional changes consistent with microglial activation. This suggests that changes in microglial function and state, rather than changes in cell abundance, result in changes in cross-talk patterns.

Next, we performed a functional enrichment of the genes involved in the predicted cross-talk interactions specific to each subset of donors to determine which biological pathways are disrupted in AD. Consistent with widespread perturbations of normal brain physiology in AD, we observed changes in the cellular cross-talk patterns when comparing AD donors with controls. The genes involved in cross-talk interactions predicted only in AD donors were significantly enriched (P range = 4.55×10^{-6} to 2.61×10^{-14}) for pathways associated with immune activation and migration (for example, response to transforming growth factor–β and amoeboid cell/leukocyte migration) and neuronal stress [for example, neuronal death and extracellular signal–regulated kinase 1/2 (ERK1/2) cascade; fig. S1C]. We also observed enrichment pattern differences across AD subtypes, such as a significant increase in ephrin signaling in ADAD donors (P range = 4.55×10^{-6} to 2.61×10^{-14}), previously linked to neuroinflammation (*5*), and more pronounced immune signaling dysregulation in *TREM2* risk variant carriers (fig. S1D). These findings suggest that global and AD subtype–specific dysregulation contributes to disease onset.

Aiming to understand how each cell type likely contributes to the dysregulated pathways in AD more generally, we performed a functional enrichment analysis separately for the cross-talk interactions detected in each cell type in cases versus controls. We observed that cross-talk interactions involving other cell types besides microglia and neurons were enriched for the very same immune activation and impaired neuronal homeostasis pathways identified in cases versus controls, further supporting that cellular cross-talk contributes to these core features of neurodegeneration (Fig. 1C). Together, these results indicate that AD leads to widespread dysregulation of homeostatic cellular cross-talk signaling pathways between microglia and neurons with other cells.

Neuron-microglia cross-talk interactions are enriched to involve known AD risk genes as ligands or receptors

Our initial analysis yielded a vast array of data, predicting thousands of cross-talk interactions across all cell types (Fig. 1B). The enormity of these data presented a challenge in discerning the precise role of cellular cross-talk in AD. To render this task more tractable and align it closely with understanding AD biology, we subsequently concentrated our analysis on interactions involving genes empirically linked to AD through genetic and functional studies. We identified 90 possible cross-talk interactions directly involving an AD gene as the ligand or receptor (table S3). Of these, 34 were detected by CellPhoneDB analyses in at least one cell type pair (Fig. 1D). We calculated, for each cell type, the association with cross-talk interactions involving AD genes using a logistic regression approach (see Materials and Methods). Microglia had the highest association for cross-talk

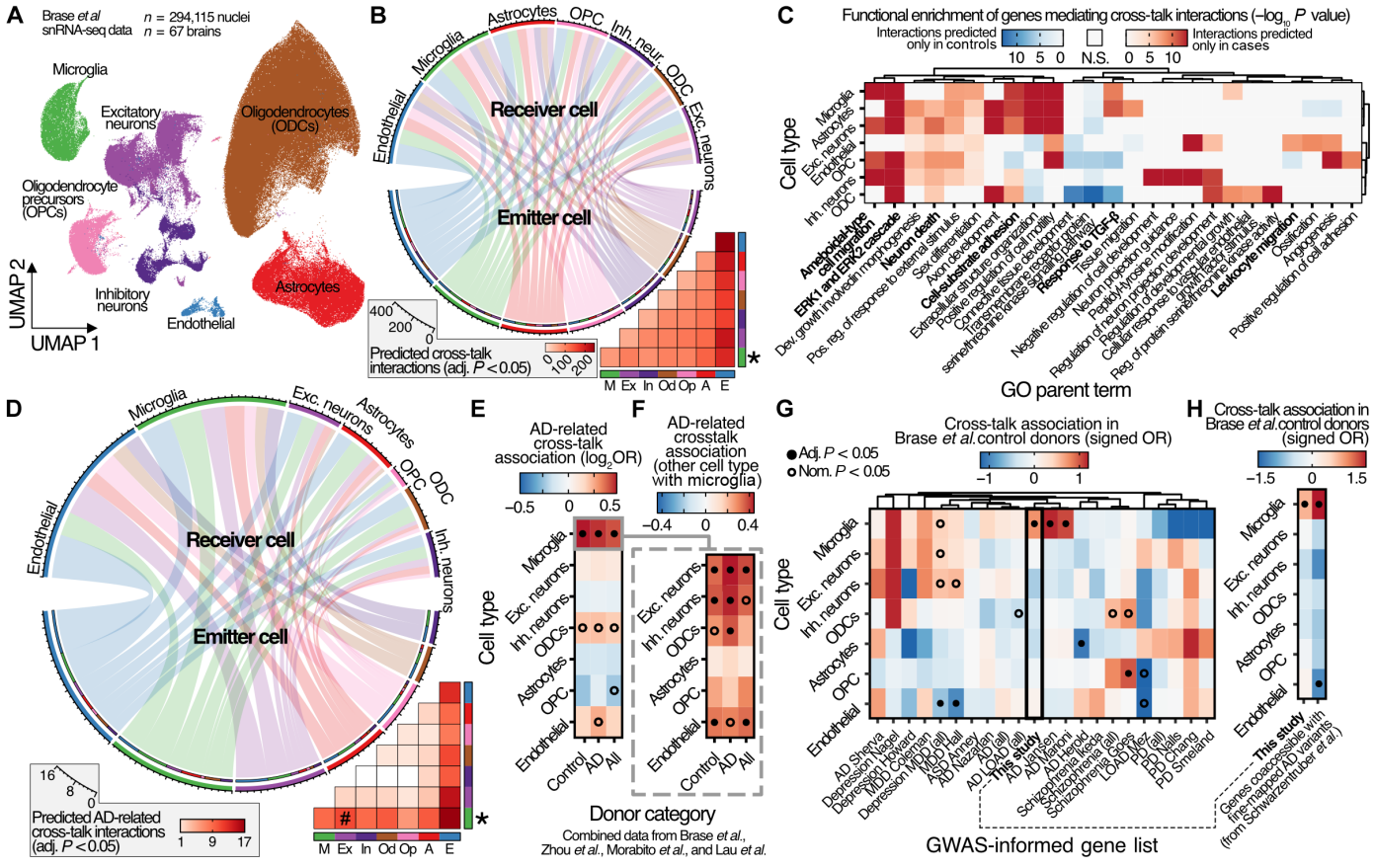

Fig. 1. Overview of predicted cellular cross-talk interactions in human brains. (**A**) Uniform Manifold Approximation and Projection (UMAP) representation of the snRNA-seq dataset identifying the seven major brain cell types from AD and control parietal cortex investigated in this study. (**B**) Chord diagram summarizing CellPhoneDB interactions derived from snRNA-seq data as in (A). The total number of unique significant CellPhoneDB interactions (Bonferroni-corrected $P < 0.05$) detected involving each cell type as either the ligand or receptor across donor categories (AD and controls) is indicated by the width of each link. Heatmap: Matrix representation of the of the same interaction data. M, microglia; Exc. neurons or Ex, excitatory neurons; Inh. neur. or In, inhibitory neurons; ODC or Od, oligodendrocytes; Op, OPCs; A, astrocytes; E, endothelial cells. Asterisks indicate cell types with significant (Fisher's exact test, $P < 0.05$) changes in the number of predicted cross-talk interactions comparing cases and controls (from fig. S1B). adj., adjusted. (**C**) Gene ontology enrichments of genes mediating cross-talk interactions only detected in cases (red colors) and controls (blue colors). N.S., not significant; TGF-β, transforming growth factor–β; GO, Gene Ontology. (**D**) Cellular cross-talk interactions involving one AD gene as either ligand or receptor across all cell type pairs. Asterisks and pound signs indicate cell types and cell type pairs, respectively, with significantly higher AD-related interactions than expected on the basis of their total number of interactions (Fisher's exact test, $P < 0.05$). (**E**) Association of AD cross-talk interactions for each cell type using combined data from multiple snRNA-seq datasets. OR, Fisher's Exact test odds ratio. (**F**) Association of AD cross-talk interactions between microglia and other cell types. (**G**) Cross-talk associations for each cell type (control donors from this study) in genes nominated by GWASs from multiple neuropsychiatric traits. MDD, major depressive disorder; LOAD, late-onset AD. (**H**) Similar to (G) but using only AD genes supported by snATAC-seq coaccessibility (see Materials and Methods).

interactions involving AD genes across all cell types regardless of which donor subset we analyzed (association range = 0.25 to 0.68, P range = 0.015 to 3.53×10^{-3}; Fig. 1E and fig. S2A). Most AD gene interactions (64.9%) were predicted to involve receptors in microglia (table S2). This observation implies that disease-associated alterations in other cells modulate a subset of AD genes in microglia.

To further understand these patterns, we explored the cell types most likely to interact with microglia through cross-talk interactions involving AD genes. We calculated the association of cross-talk interactions involving AD genes for microglial interactions with each cell type. We found that excitatory neurons displayed the highest association with microglia for these interactions (association range = 0.60 to 1.12, P range = 0.042 to 1.11×10^{-3}; fig. S2B). To further validate our findings, we leveraged data from three additional case-control snRNA-seq studies to perform a joint analysis (mega-analysis). These datasets were drawn from the prefrontal cortex region and sourced from the South West Dementia Brain Bank (SWDBB), the Rush ADRC, and the University of California Irvine Institute for Memory Impairments and Neurological Disorders (UCI MIND) ADRC (table S4) (*16*, *17*, *22*). We observed the same consistent, strong association of microglia with AD-related cross-talk interactions in each study individually and in combination (association range = 0.24 to 0.68, median = 0.53, P range = 0.022 to 3.49×10^{-4}, median = 6.17×10^{-3}; Fig. 1F and fig. S2A). We also observed the strongest association of cross-talk interactions involving AD genes for microglia with inhibitory and excitatory neurons (association range = 0.34 to 0.44, P range = 4.07×10^{-4} to 3.38×10^{-3}; Fig. 1G), as well as weaker associations with oligodendrocytes and endothelial cells. Among the

individual studies, we observed some variability concerning which type of broad neuronal cell (excitatory or inhibitory) had the highest association for interactions with microglia involving AD genes (fig. S2B), which may reflect power differences due to cell type representation. Together, our findings highlight similar overarching patterns across cohorts and brain regions. This convergence of results suggests that a subset of genes previously linked with AD may facilitate cell signaling pathways between neurons and microglia.

Cellular cross-talk pattern predictions are robust to cell representation and other potential confounding factors

To determine that our previous results were not driven by the cell type composition of the datasets, the higher representation of AD genes in microglia compared with other cell types, or other possible confounding factors, we statistically controlled for different potential sources of bias in our analyses. First, we observed that the global cross-talk patterns remained similar with dataset downsampling, including removing a subset of donors, using a single donor, using at most 100 nuclei per snRNA-seq cluster, and controlling for ambient RNA contamination (fraction of replication = 0.81 to 0.86, median = 0.84; fig. S3, A to E). We compared males versus females separately and observed an overall high degree of agreement (fraction of replication = 0.74; fig. S3F), despite a subset of interactions with likely sex-specific patterns ($n = 396$), such as Erb-B2 receptor tyrosine kinase 4 (ERBB4) and neuroregulin 1 (NRG1), which was previously linked to sexual dimorphism in the brain (*23*). These results indicate that the cross-talk interaction patterns identified using CellPhoneDB are robust to the number of donors, skews in donor representation, cell type representation, number of nuclei, sample preparation, and sequencing depth.

Next, we tested whether microglia expressed more genes present in the CellPhoneDB database and whether this could confound our findings. We observed that microglia and endothelial cells expressed more genes listed as putative ligands or receptors in CellPhoneDB (fig. S3G). However, despite more genes associated with cross-talk interactions being expressed in microglia, we did not observe an overrepresentation of AD genes participating in microglial cross-talk interactions compared to other cell types (fig. S3H). To address this potential confounding factor directly, we repeated the CellPhoneDB analyses, omitting microglia from the dataset. We observed a high concordance between the interactions detected in the complete dataset (median Spearman's ρ across donor groups = 0.988; fig. S3I).

In parallel, we calculated the enrichment of cross-talk interactions in genes nominated by GWASs for other neurological or neuropsychiatric traits (table S5). We only used cross-talk interactions predicted using the control donors from this study to make results comparable across traits. This approach is an orthogonal strategy to determine whether the abundance of microglial genes in the CellPhoneDB database skewed our previous enrichment results. We reasoned that if the cross-talk interactions observed in this study were biased toward microglia or other cell types because of database overrepresentation, then we would observe skewed enrichment patterns across traits. On the contrary, we observed distinct cross-talk enrichment patterns across neuropsychiatric traits (Fig. 1G). For example, cross-talk interactions involving OPCs were significantly associated with genes from one schizophrenia GWAS ($\log_2$ odds ratio = 1.00, adjusted $P = 0.007$). We also observed a nominally significant association for inhibitory neurons in genes identified in one major depressive disorder GWAS ($\log_2$ odds ratio = 0.57, $P = 0.02$). We furthermore replicated the enrichment for microglial cross-talk interactions in genes from two AD GWASs [Jansen *et al.* (*24*) and Marioni *et al.* (*25*), $\log_2$ odds ratios = 1.16 and 1.05, adjusted $P = 0.016$ and 0.006, respectively]. We also did not observe a skew toward microglia or endothelial cells in any of the other traits, despite these two cell types expressing more genes participating in CellPhoneDB interactions.

We further tested whether the cohort selection could confound the cross-talk analyses by repeating these analyses in a publicly available Parkinson's disease (PD) snRNA-seq dataset (see Materials and Methods). We observed distinct enrichment patterns for PD-related genes compared with AD-related genes, including a higher enrichment of PD-related cross-talk interactions in astrocytes (fig. S3J), which are in line with the baseline PD enrichment patterns we observed in our dataset (Fig. 1G). We compared the cross-talk patterns across all four AD and the PD snRNA-seq datasets and observed a high correlation of the trait-related enrichment patterns across all datasets and cell types (median Pearson's $\rho = 0.69$, $P \leq 7.43 \times 10^{-5}$; fig. S3K). These results confirm that the cross-talk enrichment patterns across cell types are highly specific to each neuropsychiatric trait and robust to cohort differences.

Last, we addressed the potential for bias resulting from the selection of candidate AD genes for our cross-talk analyses. The complex task of identifying causal genes in AD GWASs can hinder the accurate determination of cell types mediating AD genetic risk at individual loci. In addition, the possibility of nominating multiple genes within the same locus, likely participating in similar pathways (for example, the MS4A locus) (*26*), could lead to overrepresentation ("double counting") of the same GWAS signal. To mitigate these biases, we adopted a data-driven approach for nominating AD genes, relying strictly on cell type–specific chromatin coaccessibility between gene promoter regions and a fine-mapped AD GWAS variant (*12*) or the direct overlap of fine-mapped variants at the gene promoter region (see Materials and Methods). This stringent approach nominates candidate AD genes and their corresponding cell types solely on the basis of direct evidence from a brain single-nucleus assay for transposase-accessible chromatin (snATAC-seq) dataset (*17*). Despite microglia being among the least abundant cell types in the snATAC-seq dataset analyzed, we observed a twofold higher enrichment for microglial cross-talk interactions in AD compared with using our original AD genes list ($\log_2$ odds ratio = 1.51, $P = 1.89 \times 10^{-4}$; Fig. 1H). This result shows that the enrichment of AD-related cross-talk interactions is robust to varying degrees of stringency in the strategy for selecting candidate AD genes and independently recapitulates the well-established role of microglia in mediating AD genetic risk.

Combined, these results indicate that the observed cross-talk enrichment patterns are robust to potential technical confounding factors and database biases. Furthermore, these analyses highlight that our cross-talk framework is highly flexible and can be extended to understand biological processes associated with other neurological and neuropsychiatric diseases.

Microglia-neuron cross-talk interactions regulate additional known AD genes in microglia

Given our previous results prioritizing neuron-microglia cross-talk interactions in AD, we sought to investigate how the cross-talk signals between neurons and microglia could regulate gene regulatory networks downstream in microglia. Using a system biology approach

based on extending the functionality of the CytoTalk software (*27*) (see Materials and Methods), we reconstructed the gene coexpression networks upstream of the cross-talk ligands and downstream of the receptors. CytoTalk is complementary to CellPhoneDB, because the latter does not inform the biological processes likely downstream of cross-talk interactions. In addition, CytoTalk prioritizes cross-talk interactions on the basis of their predicted regulatory impact on the coexpression network topology (prioritizing interaction ligands and receptors coexpressed with central genes in the network). We did not restrict the cross-talk interactions in CytoTalk to those involving AD genes to allow an unbiased cross-talk prioritization. This way, any AD-related cross-talk interactions prioritized by CytoTalk directly reflect their predicted importance in modulating central genes in their respective coexpression networks.

We reconstructed the gene regulatory network associated with cross-talk interactions between excitatory neurons and microglia for each donor category, which was then combined into a single network to help understand the broader biological processes likely regulated by neuron-microglia cross-talk (Fig. 2, A and B). We observed similar cross-talk network topologies across excitatory and inhibitory neurons, which suggests shared signaling pathways mediating their interactions with microglia (Fig. 2A and fig. S4A). We focused on excitatory neurons because they had the highest association of AD-related cross-talk interactions with microglia and were the most represented neuronal type in our data (Fig. 1, A and F), thus increasing our confidence in the inferred coexpression networks. The microglial coexpression network downstream of the prioritized neuron-microglia cross-talk interactions was enriched for genes previously associated with AD, even after statistically accounting for the overrepresentation of AD-related genes expressed in microglia (see Materials and Methods; case odds ratio = 3.50, adjusted $P = 3.92 \times 10^{-5}$; Fig. 2C). The microglial component of the cross-talk network identified by CytoTalk was enriched for immune processes, including phagocytosis and cytokine production (Fig. 2D), consistent with neuron-microglia cross-talk interactions modulating microglial activation states (*28*). These results suggest that neuron-microglia cross-talk interactions propagate signals that modulate genes previously implicated in AD and involved in regulating microglial activation.

Among the seven cross-talk interactions prioritized by CytoTalk based on the coexpression network topology, we identified the interaction between the neuronal ligand SEMA6D and TREM2/transmembrane immune signaling adaptor (TYROBP; DNAX–activation protein 12; DAP12) (Fig. 2B). This cross-talk interaction was initially described in the context of peripheral myeloid cells activation (*29*), but its role in microglia and AD remains unknown. Given the central role of TREM2 in AD genetic risk, this notable knowledge gap motivated us to pursue this interaction further.

The TREM2-SEMA6D cross-talk is mediated by plexin A1 (PLXNA1) (*29*). Because of the low detection rate and limited dynamic range of *PLXNA1* in the snRNA-seq data (only about 10% of microglia had detectable *PLXNA1* transcript levels; maximum *PLXNA1* expression = 3 reads; fig. S5), *PLXNA1* was not included in the CytoTalk-reconstructed network. This is a reported limitation of snRNA-seq for lowly expressed genes (*30*, *31*) and precluded the reconstruction of the *PLXNA1* coexpression network by CytoTalk, resulting in a direct link between *SEMA6D* and *TREM2/TYROBP* in the excitatory neuron-microglia network. Nonetheless, microglial *PLXNA1* and neuronal *SEMA6D* expression patterns were sufficiently specific for both CellPhoneDB and CytoTalk to independently detect and prioritize the SEMA6D-PLXNA1/TREM2 cross-talk interaction between microglia and neurons in our analyses.

The SEMA6D-TREM2 cross-talk axis is predicted to modulate microglial activation

We next sought to understand how the TREM2-SEMA6D cross-talk interaction could regulate microglial biology. We identified a subnetwork composed of genes highly connected to *TREM2* and *TYROBP* by partitioning the microglial cross-talk network into subnetworks (see Materials and Methods). Our cross-talk network reconstruction analysis predicted that this *TREM2* subnetwork is the target of neuronal SEMA6D (Fig. 2E). Furthermore, the *TREM2* subnetwork was enriched for microglial activation pathways, indicating that this unsupervised approach recapitulated the well-established link between TREM2 and microglial activation (Fig. 2D) (*32*). In addition to genes linked to microglial activation, the TREM2 cross-talk subnetwork included *APOE* and *HLA* genes, previously reported as AD risk genes. The coexpression of *TREM2* and *APOE* is consistent with studies showing that apolipoprotein E (apoE) is a TREM2 ligand (*33*, *34*). These results suggest that the TREM2-SEMA6D cross-talk interaction modulates AD risk genes in microglia and is a core feature of neuron-microglia communication.

To validate these findings, we repeated the CytoTalk analyses in the snRNA-seq studies from the SWDBB, Rush ADRC, and UCI MIND ADRC cohorts (*16*, *17*, *22*). Consistent with our results, CytoTalk prioritized the SEMA6D-TREM2 signaling axis mediating the cross-talk interactions between excitatory neurons and microglia in all three cohorts, as well as identifying a similar *TREM2* subnetwork in all but one of the datasets (fig. S4B). Last, we determined that the *TREM2* subnetwork and its predicted modulation by SEMA6D were robust to the choice of donors and the number of nuclei used to reconstruct the cross-talk network (fig. S4C). Together, these results reinforce that the unsupervised methodological approach in this study identified core elements of microglial gene regulation, which are predicted to be modulated by neuron-microglia cellular cross-talk interactions.

The microglial *TREM2* subnetwork expression is impaired at late AD stages

We next determined how the *TREM2* subnetwork related to AD progression. We leveraged the wide range of neuropathological states in our dataset to develop a statistical framework to test the association of this subnetwork gene expression with disease severity while controlling for genetic and other confounding factors (see Materials and Methods). By analyzing gene expression at the level of gene subnetworks, this approach also helped mitigate data sparsity in snRNA-seq differential expression analysis. Given the comprehensiveness of Braak staging among the neuropathological annotations within our cohort, we used a high Braak stage (Braak ≥ IV) as a surrogate of AD severity. The expression of the *TREM2* subnetwork was negatively associated with high Braak stage ($\beta = -0.31$, adjusted $P = 4.32 \times 10^{-57}$), indicating that this subnetwork is down-regulated in later AD stages. To understand this result within the broader context of all neuron-microglia cross-talk interactions, we calculated the association of all neuron-microglia cross-talk subnetworks with high Braak stage. Most (11 of 14) of the microglial cross-talk subnetworks were negatively associated with high Braak stage, and the *TREM2* subnetwork was among the most negatively associated with high Braak stage (Fig. 2F). These results suggest that neuron-microglia cross-talk interactions

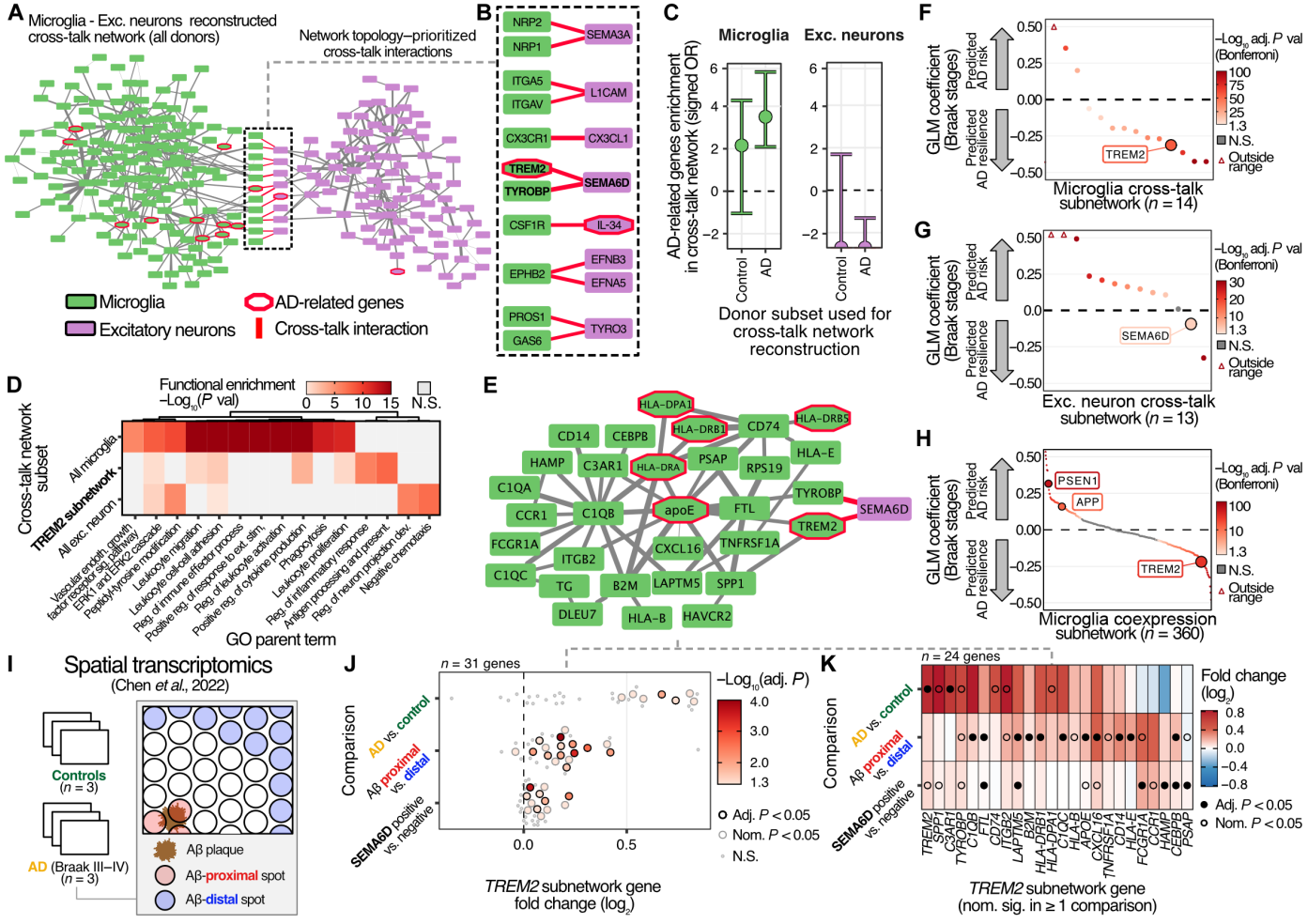

Fig. 2. Cross-talk interactions between neurons and microglia are predicted to modulate AD risk genes. (**A**) Microglia–excitatory neuron cross-talk network inferred by CytoTalk. (**B**) Independently prioritized cross-talk interactions using CytoTalk. (**C**) Enrichment of AD genes in the microglial cross-talk network across donor categories. (**D**) Gene ontology enrichments for the genes participating in cross-talk networks of microglia and excitatory neurons. (**E**) Predicted TREM2 cross-talk subnetwork. (**F**) Association of microglial cross-talk subnetworks (individual points) with high Braak stage. GLM, generalized linear model. (**G**) Association of excitatory neuronal cross-talk subnetworks with high Braak stage. (**H**) Association of all microglial subnetworks with Braak stage. (**I**) Spatial transcriptomics validation cohort overview. (**J**) Changes in gene expression in the TREM2 cross-talk subnetwork associated with disease status, Aβ plaque proximity, and presence of SEMA6D-expressing cells. (**K**) Individual gene view for comparisons in (J).

and their downstream targets in microglia are impaired in the later stages of AD.

Next, we determined whether SEMA6D is a potential modulator of the *TREM2* microglial cross-talk subnetwork. We reasoned that if this were the case, then the neuronal *SEMA6D* cross-talk subnetwork association with high Braak stages would agree in direction with the *TREM2* subnetwork. The neuronal *SEMA6D* subnetwork was also negatively associated with high Braak stage ($\beta = -0.09$, adjusted $P = 1.63 \times 10^{-4}$; Fig. 2G). Therefore, our findings indicate that the biological processes involved in the SEMA6D-TREM2 neuron-microglia cross-talk interactions are disrupted in AD and likely play a protective role by regulating TREM2-dependent microglial activation.

Multiple microglial coexpression subnetworks are disrupted during AD progression

To gain further insights into the role of microglia in AD, we next adapted the network analysis framework of CytoTalk to analyze the transcriptome-wide microglial coexpression network (using all expressed genes in microglia instead of the subset prioritized by CytoTalk; see Materials and Methods). This approach allowed us to test the association of all microglial subnetworks with high Braak stage, regardless of the presence of reported ligands/receptors in the subnetworks. We partitioned the full microglial coexpression network into 360 subnetworks and independently recapitulated several subnetworks from the previous cross-talk–prioritized network reconstruction, including the *TREM2* subnetwork (fig. S6, A to C). These microglial subnetworks were divided between positive and negative associations with high Braak stage (Fig. 2H and table S6). Consistent with the well-established roles of presenilin 1 (PSEN1) and amyloid beta precursor protein (APP) in AD onset (*35*), the *PSEN1* and *APP* coexpression subnetworks were among the most positively correlated with high Braak stage ($\beta = 0.32$ and 0.16, adjusted $P = 8.25 \times 10^{-57}$ and 2.17×10^{-13}, respectively). In contrast, the subnetwork of *SORL1*, a gene associated with protective roles in AD (*36*, *37*), was negatively associated with Braak

stage ($\beta = -0.15$, adjusted $P = 3.52 \times 10^{-11}$). Our unsupervised approach identified two separate subnetworks with opposing directions of effect for the genes in the MS4A locus, which genetically controls soluble TREM2 expression (*26*) (*MS4A4A* and *MS4A6A*, $\beta = -0.11$ and 0.19, adjusted $P = 2.87 \times 10^{-6}$ and 2.93×10^{-20}, respectively). This result suggests that the MS4A genetic signal regulates at least two independent biological processes, consistent with what we reported in a previous study (*26*). Within the context of all microglial genes, the *TREM2* subnetwork was among the most negatively associated with Braak stage (Fig. 2H), consistent with our analysis of the cross-talk–prioritized network. These results indicate that multiple biological pathways downstream of microglia-neuron cross-talk are disrupted in AD. Furthermore, our unsupervised computational framework identified impaired TREM2-dependent microglial activation associated with AD progression.

The TREM2 subnetwork expression correlates with proximity to Aβ plaques and is up-regulated in the presence of SEMA6D

Our findings that the *TREM2* subnetwork was among the most negatively associated with advanced AD stages motivated us to better understand how its expression changed as a function of neuropathological burden. To do so, we reanalyzed three control and three AD (Braak III and IV) human brains (*38*) using spatial transcriptomics (10x Genomics Visium). We quantified the effects of local neuropathology, particularly proximity to Aβ plaques, on gene expression patterns (Fig. 2I).

We first analyzed the global changes in gene expression between AD cases and controls and identified only 7 of 31 genes in the *TREM2* subnetwork with a nominally significant association (median $\log_2$ fold change = 0.67, adjusted $P < 0.05$; Fig. 2, J and K). However, when we compared Aβ plaque–proximal to Aβ plaque–distal regions, we observed an up-regulation of most genes in the *TREM2* subnetwork (17 of 31 genes at least nominally significant; median $\log_2$ fold change = 0.18, adjusted $P < 0.05$). The spatially resolved data also showed a progressive up-regulation of genes in the *TREM2* subnetwork as a function of Aβ plaque proximity (fig. S7, A and B), indicating that this pathway is likely involved in the immune response to amyloid pathology. Supporting this hypothesis, we observed that other gene signatures linked to plaque-associated microglia in single-cell transcriptomics studies of AD mouse models (*15*, *39*) were also up-regulated with Aβ proximity (fig. S7C).

Last, we leveraged the resolved spatial relationship of this dataset to test whether the *TREM2* subnetwork expression changed in proximity to *SEMA6D*-expressing cells. In line with our single-cell analyses, we observed a significant up-regulation of the *TREM2* subnetwork when comparing *SEMA6D*-positive versus *SEMA6D*-negative spots (19 of 31 genes at least nominally significant; median $\log_2$ fold change = 0.081, adjusted $P < 0.05$; Fig. 2, J and K). *TREM2* subnetwork activation in proximity to *SEMA6D* was comparable between cases and controls (fig. S7D). These results, combined with the lower expression of the *TREM2* subnetwork in the high Braak stage donors from the snRNA-seq data (Fig. 2H), suggest that the *TREM2* cross-talk subnetwork is active during earlier Braak stages and responds to local neuropathology (Aβ plaques) and SEMA6D signaling but loses function as the disease progresses. Our findings suggest that the *TREM2* subnetwork is involved in the response to Aβ plaques and is activated by SEMA6D.

SEMA6D colocalizes with Aβ plaques in human AD brains and associates with TREM2-activated microglia in early but not late AD stages

Our snRNA-seq and spatial transcriptomics analyses independently suggested that SEMA6D activates the TREM2 subnetwork in microglia near Aβ plaques and that this subnetwork loses function during advanced disease stages. To validate this hypothesis, we performed quantitative cyclic multiplex immunofluorescent imaging of TREM2, SEMA6D, PLXNA1, and Aβ in human brains across different stages of AD progression (control, Braak stage IV, and Braak stage V/VI; Fig. 3, A to D, and fig. S8, A to H).

We observed that SEMA6D was almost exclusively detected in the vicinity of Aβ plaques (Fig. 3, A to C, and fig. S8), which we confirmed by comparing Aβ plaque–proximal versus Aβ plaque–distal regions ($P = 3.18 \times 10^{-14}$; Fig. 3, E and F, and fig. S8G). In addition, the SEMA6D signal associated with multiple cell types in the vicinity of Aβ plaques, including neurons, astrocytes, and microglia (Fig. 3 and fig. S8, I and J), suggesting a complex cellular landscape of this signaling pathway in the AD brain microenvironment. In parallel, we observed a significant increase in TREM2 microglia near plaques ($P = 2.12 \times 10^{-9}$; Fig. 3G and fig. S8C). We furthermore observed a significant shift in microglia from a TREM2-activated to a homeostatic-like phenotype, marked by higher transmembrane protein 119 (TMEM119) expression, when comparing the intermediary versus late Braak stages ($P = 1.73 \times 10^{-9}$; Fig. 3, G to I, and fig. S8, C and D). We also observed a significant, albeit less pronounced, decrease in Aβ-proximal SEMA6D expression when comparing intermediary versus late Braak stages ($P = 0.032$; Fig. 3F and fig. S8G), suggesting that this signaling is impaired with disease progression. We observed poor colocalization of PLXNA1 with SEMA6D, which could indicate other co-receptors mediate the TREM2-SEMA6D interaction. Together, these observations align with our transcriptomics findings and further support our hypothesis that SEMA6D induces microglial activation near Aβ plaques and our computational prediction that the TREM2 transcriptional subnetwork is impaired at late AD stages.

SEMA6D induces immune activation in iMGL in a TREM2-dependent manner

To elucidate the role of SEMA6D-TREM2 cross-talk in microglial function, we used a human iMGL model (*40*) (fig. S9A and Materials and Methods) that expresses established microglial markers by immunofluorescence, including TREM2, ionized calcium-binding adaptor molecule 1 (IBA-1), and TMEM119 (fig. S9B). In addition, we generated *TREM2* KO human iPSCs using CRISPR-Cas9 to examine the role of the SEMA6D-TREM2 signaling axis on microglial function (fig. S9C). We verified the loss of TREM2 expression at the protein level in the KO cell line by Western blot analysis (fig. S9D). By flow cytometry, we verified that the iMGL express key microglial markers such as CD11b, CD45, and TREM2 (fig. S9, E to H).

Because microglia regulate brain homeostasis through phagocytic activity and modulate neuroinflammation by releasing immune cytokines (*41*–*43*), we performed kinetic phagocytosis and cytokine release assays to verify iMGL function. We demonstrated that iMGL phagocytose both pHrodo-labeled human synaptosomes and Aβ oligomers, as quantified by fluorescent total integrated intensity (fig. S10, A to D). Cytochalasin D was used as a negative control for phagocytosis activity (fig. S10D). To determine whether SEMA6D can regulate iMGL phagocytic activity and whether this process is

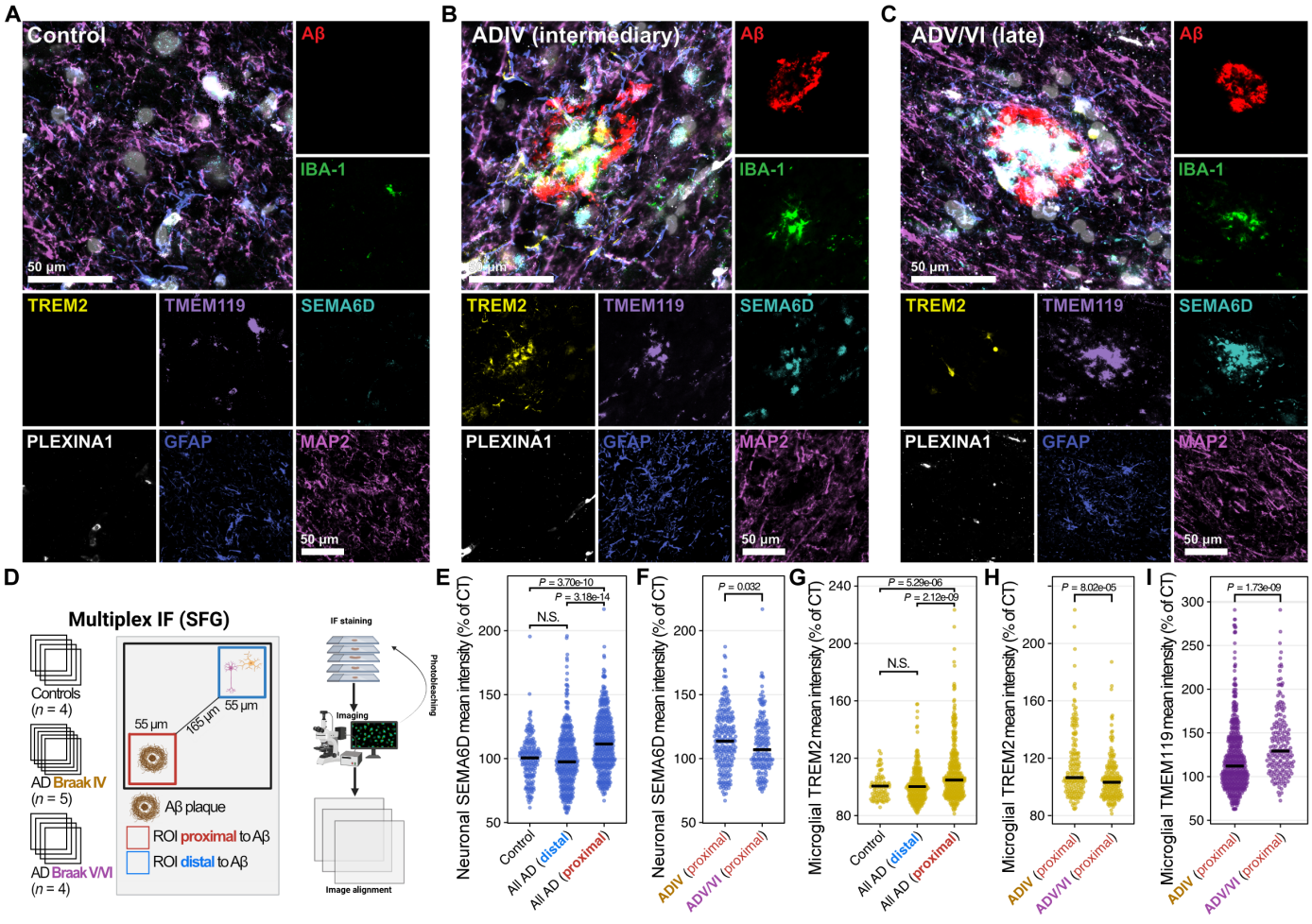

Fig. 3. SEMA6D cooccurs with Aβ plaques and TREM2-activated microglia during early AD stages and with Aβ plaques and "homeostatic-like" microglia in late AD stages. (**A** to **C**), Representative images of cyclic multiplex immunofluorescence imaging of (A) control (B) AD Braak stage IV (ADIV) proximal, and (C) AD Braak stage V/VI (ADV/VI) proximal. The cyclic multiplex staining was performed as follows: round 1 (R1): TREM2 (pseudo-yellow), TMEM119 (pseudo-lavender), and PLXNA1 (pseudo-white); R2: IBA-1 (pseudo-green) and glial fibrillary acidic protein (GFAP; pseudo-blue); R3: Aβ (pseudo-red) and SEMA6D (pseudo-teal); R4: microtubule associated protein 2 (MAP2; pseudo-pink). Nuclei for all rounds were visualized using Hoechst33342 (gray in the merged image). Scale bars, 50 μm. (**D**) Cyclic multiplex immunofluorescence (IF) experiment workflow. SFG, superior frontal gyrus. (**E** and **F**) Quantification of the mean intensity of SEMA6D within individual neurons (MAP2$^+$) comparing controls to combined AD proximal and distal (E) and individual ADIV and ADV/VI proximal (F). (**G** and **H**) Quantification of the mean intensity of TREM2 within individual microglia/macrophages (IBA-1$^+$/TMEM119$^+$) comparing controls to combined AD proximal and distal (G) and individual ADIV and ADV/VI proximal (H). (**I**) Quantification of the mean intensity of TMEM119 within individual microglia/macrophages (IBA-1$^+$/TMEM119$^+$) compared to ADIV proximal and ADV/VI proximal. All comparisons were made with a Wilcoxon rank sum test using Bonferroni multiple testing correction.

TREM2 dependent, we treated WT and *TREM2* KO iMGL with recombinant SEMA6D protein. We measured the degree of phagocytic activity using pHrodo-labeled human synaptosomes as the phagocytic cargo. We used human brain-derived synaptosomes as the substrate because they are a physiologically relevant microglial phagocytic cargo and would not confound our results with any potential innate activating effects from Aβ. In three independent experiments (fig. S11A), we observed increased phagocytosis in WT iMGL treated with SEMA6D starting at 6 hours of treatment with SEMA6D (1.3-fold change increase at 24 hours relative to untreated, $P = 0.0035$, linear mixed-effects model). In contrast, *TREM2* KO iMGL treated with SEMA6D had an insignificant increase in phagocytosis compared to untreated *TREM2* KO cells (1.1-fold change at 24 hours relative to untreated, $P = 0.29$; Fig. 4, A and B, and fig. S11A) and showed abrogated phagocytosis compared with WT-treated cells. In parallel, we analyzed conditioned medium of WT and *TREM2* KO iMGL using a multiplex immunoassay to determine whether SEMA6D can regulate iMGL cytokine release. SEMA6D increased the secretion of tumor necrosis factor–α (TNF-α) and interleukin-6 (IL-6) in WT but not *TREM2* KO iMGL (WT TNF-α and IL-6, fold changes = 1.37 and 3.59, $P = 4.58 \times 10^{-5}$ and 3.11×10^{-5}, respectively; Fig. 4C). We replicated the effects of SEMA6D treatment in iMGL generated from an independent WT isogenic iPSC line, indicating that the observed effects of SEMA6D treatment in iMGL activation were not due to cell line–specific effects (fig. S11, B and C). Together, these results indicate that SEMA6D increases iMGL phagocytosis and secretion of TNF-α and IL-6 cytokines in a primarily TREM2-dependent manner.

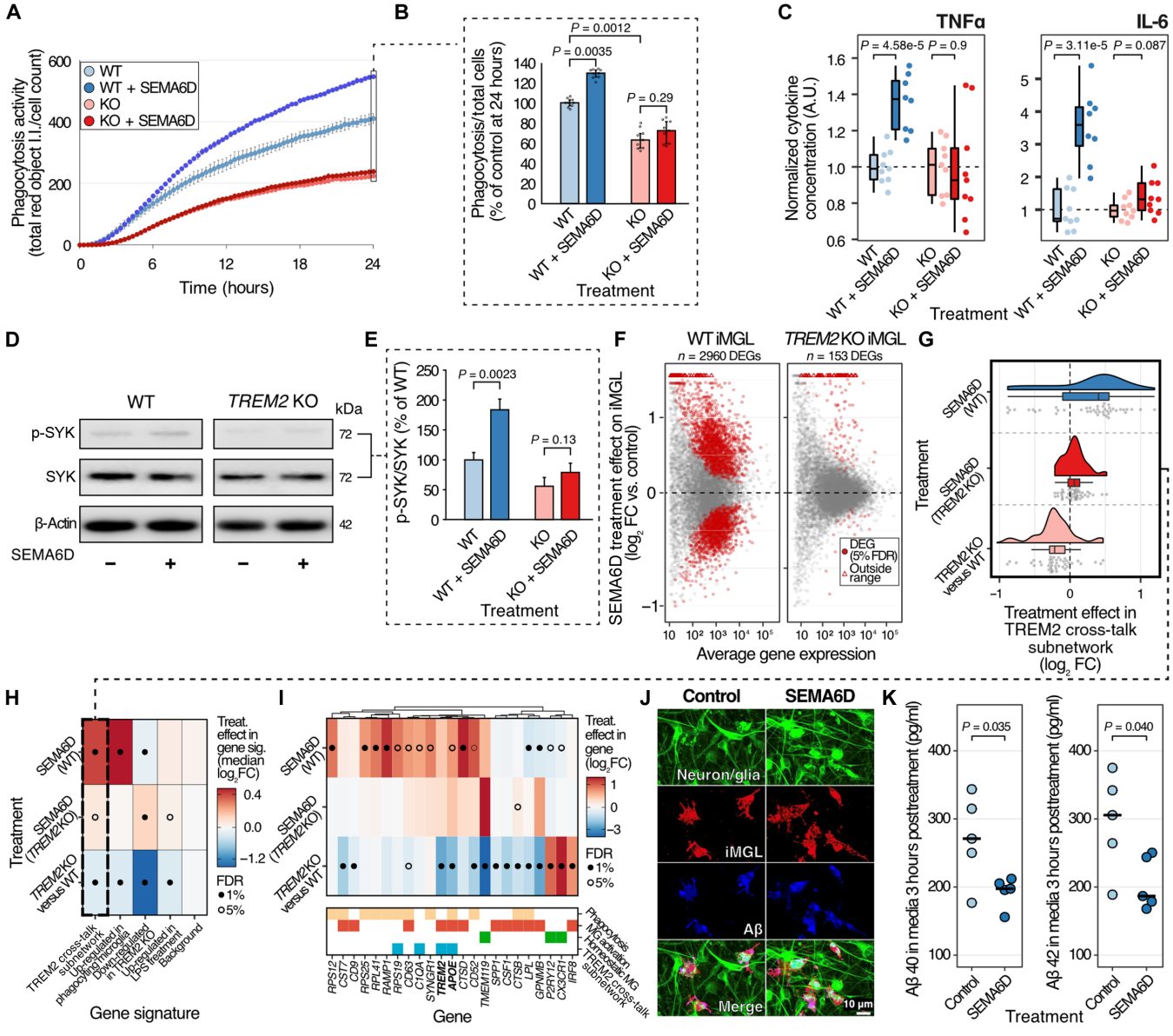

Fig. 4. SEMA6D treatment induces microglial activation in a TREM2-dependent manner. (**A**) Phagocytosis of synaptosomes by WT or TREM2 KO iMGL treated with SEMA6D (10 μM). *y* axis shows total well red fluorescent integrated intensity (I.I.). Data were averaged from three independent experiments (shown in fig. S11A); means ± SD. (**B**) Quantification of phagocytosis of synaptosomes by WT or TREM2 KO iMGL treated with SEMA6D at 24 hours. Data represent the three independent experiments performed in triplicate; median ± interquartile values at 24 hours. *P* values were obtained from using a linear mixed-effects model (shown in fig. S11A). (**C**) Quantification of TNF-α and IL-6 in medium from WT or TREM2 KO iMGL treated with SEMA6D (10 μM), using the Mesoscale V-plex neuroinflammation panel. Box plots indicate median and interquartile ranges. *P* values are calculated using linear regression. A.U., arbitrary units. (**D**) Representative Western blots of p-SYK and total SYK in WT and TREM2 KO iMGL treated with SEMA6D (10 μM). β-Actin was the loading control (**E**) Quantification of p-SYK/total SYK chemiluminescent Western blot analysis, $n = 3$ (individual replicates shown in fig. S12). (**F**) Bulk RNA-seq effect size distribution indicating the transcriptional changes induced by SEMA6D treatment in WT and TREM2 KO iMGL. FC, fold change; DEGs, differentially expressed genes. (**G**) Transcriptional changes in the TREM2 cross-talk subnetwork associated with SEMA6D treatment (WT or TREM2 KO versus untreated control) or TREM2 KO (TREM2 KO versus WT, no treatment). Only TREM2 subnetwork genes differentially expressed in at least one comparison are included. (**H**) Transcriptional effects of the same conditions across clinically and biologically relevant gene signatures. Background corresponds to 500 randomly selected genes. Solid dots correspond to a 1% FDR significance threshold for comparing the effect size distribution to the corresponding background (Mann-Whitney test). (**I**) Transcriptional effects of the experimental conditions across a representative subset of highly differentially expressed genes from the signatures in (H). (**J**) Representative confocal immunofluorescence of 3D triculture model consisting of differentiated ADAD hNPCs (neuron/glia-GFP, green) and iMGL (IBA-1, red), stained for Aβ (blue). (**K**) Analysis of Aβ40 and Aβ42 expression in conditioned medium of triculture model after 24 hours of pretreatments, followed by 3 hours of co-retreatments. Control IgG ($n = 5$) and SEMA6D ($n = 5$). Vertical bars, median. Unpaired two-tailed *t* test.

TREM2 mediates signaling through the adaptor protein TYROBP (DAP12), and the activation of TREM2 results in tyrosine phosphorylation within the immunoreceptor tyrosine-based activation motif and subsequent spleen tyrosine kinase (SYK) phosphorylation (*44*). To determine whether SEMA6D activates TREM2 downstream signaling, we analyzed WT and *TREM2* KO iMGL protein lysates for phosphorylated SYK expression normalized to total SYK expression. Treatment of WT iMGL with SEMA6D induced a 1.84-fold increase in SYK phosphorylation ($P = 0.0023$), but these effects were not observed in *TREM2* KO iMGL ($P = 0.13$; Fig. 4, D and E, and fig. S12). These results demonstrate that SEMA6D can directly activate TREM2 signaling and suggest that SEMA6D preferentially signals through the TREM2/TYROBP (DAP12) complex in microglia, although we cannot exclude that SEMA6D simultaneously activates other signaling pathways.

To systematically characterize the transcriptional changes induced by SEMA6D treatment in iMGL, we generated bulk RNA-seq data for the SEMA6D-treated WT and *TREM2* KO iMGL and the corresponding untreated controls (fig. S13). We observed significant transcriptional changes associated with *TREM2* KO [$n = 1408$ differentially expressed genes at 10% false discovery rate (FDR); fig. S13, A and B]. As expected, *TREM2* was among the most down-regulated genes in the *TREM2* KO iMGL (adjusted $P = 4.30 \times 10^{-22}$, rank = 26; fig. S13A). We observed robust transcriptional changes in SEMA6D-treated WT iMGL but not in SEMA6D-treated *TREM2* KO iMGL ($n = 2960$ and 153 differentially expressed genes at 10% FDR, respectively; Fig. 4F and fig. S13, A and B), consistent with a pivotal role for TREM2 in mediating SEMA6D signaling in microglia. To further understand how TREM2 mediates this signaling pathway, we focused on the *TREM2* coexpression cross-talk subnetwork predicted from the snRNA-seq data (Fig. 2E). The *TREM2* subnetwork had significantly lower expression in the untreated *TREM2* KO iMGL than WT (median $\log_2$ fold change = −0.22, adjusted $P = 4.76 \times 10^{-4}$), consistent with TREM2 being a key regulator of this subnetwork. In line with this interpretation, the *TREM2* subnetwork was activated by SEMA6D treatment in the WT iMGL (median $\log_2$ fold change = 0.40, adjusted $P = 7.50 \times 10^{-3}$) but significantly less so in the *TREM2* KO iMGL (median $\log_2$ fold change = 0.06, adjusted $P = 0.040$; Fig. 4G). These results are consistent with the TREM2 signaling pathway being the primary mediator of SEMA6D in microglia and also suggest that SEMA6D can activate other pathways to a lesser extent.

We next analyzed biologically relevant transcriptional signatures previously described in microglia to gain further insights into how SEMA6D treatment regulates microglial transcriptional programs. These included genes up-regulated in Aβ-phagocytosing microglia (*42*) and up-regulated in response to lipopolysaccharide (LPS) treatment (*18*). As control signatures, we included genes down-regulated in another *TREM2* KO iMGL dataset (*45*) and a set of randomly selected genes for which we would not expect concerted transcriptional changes (fig. S13, C and D). We observed the most substantial effects of SEMA6D treatment in the phagocytosing microglial gene signature (median $\log_2$ fold change = 0.47; Fig. 4H), indicating that SEMA6D activates genes involved in phagocytosis in the WT but not *TREM2* KO iMGL. *TREM2*, *APOE*, and *RPS19* are among the most up-regulated genes by SEMA6D treatment in WT iMGL. These genes are either present in the phagocytosing microglial gene signature or correspond to genes previously linked to microglial activation in AD mouse models (*15*, *39*) (Fig. 4I). Our results indicate that SEMA6D-TREM2 cross-talk signaling induces a TREM2-mediated cascade of transcriptional events leading to microglial activation.

SEMA6D increases Aβ clearance in a microglia-glia-neuron coculture model harboring pathogenic ADAD mutations

To investigate the role of SEMA6D on microglial Aβ clearance, we used a three-dimensional (3D) neuron-astrocyte-microglia triculture model that recapitulates AD pathology in vitro (*46*–*48*). We differentiated ReNcell VM human neural progenitor cells (hNPCs), which stably express green fluorescent protein (GFP) and the ADAD mutations APP K670N/M671L, APP V717I, and PSEN1 ΔE9 (ADAD hNPCs) in a 3D hydrogel (Matrigel) culture. Then, we added fully differentiated iMGL to the 3D-differentiated ADAD hNPCs after 4 to 6 weeks. The ADAD hNPCs differentiated into neural and glial cell 3D cultures, showing robust accumulation of Aβ species in 3D gels and microglia, detected by immunofluorescence (Fig. 4J and fig. S14A) and increased Aβ expression levels in conditioned medium (Fig. 4K).

After ADAD hNPC differentiation, we introduced iMGL to the 3D culture to determine the effects of SEMA6D on iMGL clearance of Aβ from the medium. We pretreated iMGL for 3 hours with either immunoglobulin G (IgG) Fc (control; 10 μM) or SEMA6D Fc (SEMA6D; 10 μM) and continued treatment for 3 hours after the introduction of iMGL to the 3D triculture. We did not observe changes in cell viability in this model (fig. S14, B and C). Confocal microscopy suggested Aβ uptake by iMGL as Aβ expression (anti-Aβ) colocalized with iMGL (anti–IBA1) (Fig. 4J). We quantified Aβ40 and Aβ42 in the conditioned medium by electrochemiluminescent immunoassay (Meso Scale Diagnostics). In line with our other observations, we found that SEMA6D decreased both Aβ40 and Aβ42 in the medium (Aβ40 and Aβ42, fold changes = 0.72 and 0.70, $P = 0.03$ and 0.04, respectively), suggesting that SEMA6D increases Aβ clearance by iMGL, likely by phagocytosis of soluble Aβ (Fig. 4K).

Together, our results demonstrate that SEMA6D induces a clinically relevant phenotype in this 3D human cellular model that recapitulates AD pathogenesis. These results are consistent with our spatial transcriptomics and cyclic multiplex immunofluorescent imaging findings in human AD brains.

SEMA6D is associated with AD progression in independent cohorts

To further validate our findings in independent datasets, we analyzed *SEMA6D* expression patterns in two large-scale single-nucleus transcriptomic studies from the Religious Orders Study/Memory and Aging Project (ROSMAP) and the Seattle Alzheimer's Disease Brain Cell Atlas (SEA-AD) (*49*, *50*) (fig. S15). Consistent with our observations, SEMA6D showed the highest expression in neuronal populations and was also detected at lower expression levels across multiple cell types (fig. S15, A and B). This heterogeneous expression pattern underscores the complex cellular origin of SEMA6D in the brain. When analyzing SEMA6D expression across disease progression, we observed significant positive associations with AD pathology in inhibitory ($P = 4.4 \times 10^{-3}$ in SEA-AD, $P = 4.87 \times 10^{-10}$ in ROSMAP) and excitatory ($P = 1.76 \times 10^{-3}$ in ROSMAP) neuronal populations (fig. S15, C to E).

These results from independent cohorts are consistent with our findings that SEMA6D signaling is implicated in AD pathophysiology. Further, they support that SEMA6D-TREM2 signaling represents a crucial microglial activation pathway in AD pathology.

DISCUSSION

In this study, we leveraged single-nucleus gene expression profiles from a diverse cohort of brain donors to systematically dissect the contribution of cross-cellular signaling (cellular cross-talk) networks to AD. Our data-driven approach to identifying cross-talk interactions and reconstructing their corresponding downstream pathways provides additional evidence that disrupted cellular cross-talk networks contribute to neurodegeneration. A main finding from our study is that a major portion of AD risk genes is either directly involved in cross-talk interactions or immediately downstream of cross-talk interactions involving microglia. These results highlight the difficulty of characterizing the prominent role of microglia in AD, given that the integration of complex signals originating in other brain cell types is core to their function. Specifically, our results support that dysregulation of the intricate signaling between neurons and microglia is linked to AD progression. Therefore, focusing on cellular cross-talk networks provides further functional context to understand the biology of genes associated with AD risk in a cell-autonomous and nonautonomous manner.

Among the interactions we detected between neurons and microglia, we identified a functional link between neuronal SEMA6D and microglial TREM2. Semaphorins and their receptors regulate immune cell function and are genetically and functionally implicated in AD (*51*, *52*). In the brain, semaphorin signaling was initially described as a mediator of axon guidance by the plexin family of receptors (*53*). However, a growing body of evidence indicates that these molecules are involved in immune responses (*5*, *29*, *54*–*57*). The role of SEMA6D in immune activation was described in a study showing that SEMA6D induces activation of bone marrow–derived macrophages in a TREM2- and PLXNA1-dependent manner through the activation of DAP12, consistent with the formation of a complex (*29*, *58*, *59*). Additional studies also linked semaphorin signaling to immune activation and neurodegeneration (*5*, *55*, *57*, *60*, *61*). Despite the role of SEMA6D in TREM2-dependent immune activation of peripheral myeloid cells being described almost 2 decades ago (which allowed us to computationally test this interaction in the first place) and the well-established role of TREM2 in AD genetic risk, there is a notable gap of understanding regarding this signaling pathway in the context of microglia and AD.

By leveraging iMGL, we demonstrated that SEMA6D signaling induces a TREM2-dependent microglial activation phenotype marked by increased cytokine release and Aβ phagocytosis, as evidenced by our 3D triculture brain model. Furthermore, SEMA6D-treated iMGL are transcriptionally similar to Aβ-phagocytosing microglia (*42*). In human brains, our observation that the *TREM2* coexpression subnetwork is activated in the proximity of Aβ plaques and *SEMA6D*-expressing cells, combined with our observation that the transcriptional networks upstream and downstream of the SEMA6D-TREM2 interaction are down-regulated in late AD stages, suggest that loss of this interaction exacerbates the deleterious processes occurring in the later stages of this disease. This hypothesis is supported by our multiplex immunofluorescence on human AD brains, which showed that SEMA6D is almost exclusively detected near Aβ plaques and TREM2-activated microglia, and plaque-proximal microglia switch to a homeostatic-like state at later disease stages, consistent with a recently described "exhausted" microglial subtype (*62*).

A previous study showed that SEMA6D promotes peripheral dendritic cell activation and osteoclast differentiation through the receptor complex harboring PLXNA1 and TREM2 (*29*). Thus, it is conceivable that SEMA6D functions as a natural ligand for the PLXNA1/TREM2 co-receptor and enhances TREM2 signaling in human microglia. Therefore, SEMA6D could influence functional properties by stimulating TREM2-dependent intracellular signaling and inducing the *TREM2* gene expression network. However, other studies described how SEMA6D also regulates lipid metabolism and polarization of macrophages through the interaction with another plexin, PLXNA4 (*54*, *55*). *PLXNA4* coding variants have been linked to AD risk (*55*, *63*) and found to modulate amyloid and tau pathology (*60*). Thus, semaphorin-plexin signaling may play a fundamental role in regulating the functional interactions with microglia and other cell types and may be perturbed in AD. Given that we observed a small subset of transcriptional changes in iMGL associated with SEMA6D treatment in the absence of TREM2, it is possible that other proteins, such as PLXNA4, act as secondary SEMA6D receptors in microglia. This alternative receptor hypothesis is further supported by the poor colocalization between PLXNA1 and TREM2 in the multiplex immunofluorescence on human brains, which suggests that TREM2-dependent microglial activation by SEMA6D can be achieved independently of PLXNA1. Therefore, future studies must determine the complete network of proteins mediating SEMA6D cross-talk in microglia.

Although this study focused on a restricted subset of cross-talk interactions involving microglia and neurons, our systematic characterization of cellular cross-talk signaling patterns identified thousands of candidate interactions involving all brain cell types represented in our snRNA-seq data. Several of these interactions warrant further investigation. For example, the interleukin receptor IL-1RAP has been previously implicated in genetic studies of AD endophenotypes (*3*, *64*–*66*), and the contribution of IL-1 signaling to neurodegenerative diseases is well established (*67*–*69*). In line with these studies, we identified the *IL1RAP* subnetwork in microglia as the most negatively associated with high Braak stages (table S6). These results suggest that the IL-1 signaling pathway disruption is likely involved in AD progression. More broadly, the IL-1RAP case highlights that the continued exploration of brain cross-talk networks identified in this study will yield valuable biological insights into AD biology.

Our study has limitations: Our single-cell transcriptomics analyses implicated neurons as the primary partners for microglia regarding the SEMA6D-TREM2 cross-talk interaction. However, we also observed *SEMA6D* expression to a lesser extent in non-neuronal cell types. Our multiplex immunofluorescence imaging studies could not rule out that other cell types are also associated with Aβ-proximal SEMA6D in human brains. Whereas we primarily quantified SEMA6D in neurons, we acknowledge that SEMA6D may also be expressed in other cell types near Aβ plaques, including astrocytes and potentially microglia. We note that our in vitro experiments used exogenous SEMA6D. Thus, additional experiments will be required to directly demonstrate neuron-microglia cross-talk, possibly through conditional expression of SEMA6D in neurons. To mitigate this limitation, we relied on the convergence of multiple independent methods, including snRNA-seq, spatial transcriptomics, and functional validation in *TREM2* KO cell lines to support our conclusions. Further experimental studies, including high-resolution immunostaining of neuronal projections and cell-sorting approaches, are necessary to unambiguously determine the primary cell types contributing to SEMA6D-TREM2 signaling in microglia and fully characterize the cellular sources of plaque-associated SEMA6D in human AD brain tissue. Nevertheless, the consistent spatial association of

SEMA6D with Aβ plaques across multiple brain samples and our in vitro experiments demonstrating that exogenous SEMA6D can induce TREM2-dependent microglial activation provide compelling evidence for the involvement of this signaling pathway in AD pathophysiology.

Another limitation of our study is its reliance on existing databases of curated cross-talk interactions, which exclude interactions not yet reported in the literature. Moreover, our transcriptomics-based approach may overlook cellular communication mediated by molecules synthesized through complex biochemical pathways lacking canonical ligand genes (lipids and some neurotransmitters) or not relying on a specific receptor in the conventional sense (nitric oxide signaling). Lastly, our understanding of the genetic risk of AD and other neuropsychiatric traits is incomplete. This knowledge gap hinders the discovery of yet-unknown risk genes and their corresponding cross-talk networks, precluding a complete characterization of the role of cellular cross-talk in neurodegeneration. Despite these constraints, our results indicate that a systematic characterization of cellular cross-talk networks can provide valuable insights into the biology of neurodegenerative diseases, potentially aiding in identifying new therapeutic targets. Given our findings, we advocate for developing new high-throughput assays to systematically identify cell-to-cell communication pathways.

Last, we identified unique cross-talk enrichment patterns for genes found in genetic studies of other neurological or neuropsychiatric traits. This result underscores the integral role of cellular cross-talk in normal brain physiology and suggests that acknowledging this regulatory layer will aid in understanding how candidate disease risk genes fit into broader biological pathways. Together, our findings strongly support that the systematic characterization of cellular cross-talk networks is a viable strategy for gaining insight into the biology of neurodegenerative diseases and nominating targets for future therapies.

MATERIALS AND METHODS

Study design

This study aimed to identify dysregulated signaling pathways in AD and potential therapeutic targets by analyzing snRNA-seq data from human brains using computational approaches, followed by validation using spatial transcriptomics, immunofluorescence imaging, and functional experiments in iMGL. Key treatments included treating WT and TREM2 KO microglia with SEMA6D, with measurements of phagocytic activity, cytokine release, gene expression, and protein phosphorylation to assess microglial activation and Aβ clearance, using sample sizes from established protocols in the literature without randomization or blinding. Human postmortem samples were previously obtained with informed consent for research use approved by the review board of Washington University in St. Louis, and neuropathological changes were assessed according to the National Institute on Aging-Alzheimer's Association criteria, with demographic, clinical severity, and neuropathological information available in our original study (*14*).

Statistical analyses

Statistical analyses were performed using R and GraphPad Prism. All tests were two sided, with $P < 0.05$ considered significant unless noted otherwise. Detailed statistical approaches for each analysis are provided in the Supplementary Materials.

Supplementary Materials

The PDF file includes:
Materials and Methods
Figs. S1 to S15
References (*70*–*103*)

Other Supplementary Material for this manuscript includes the following:
Tables S1 to S7
Data file S1
MDAR Reproducibility Checklist

REFERENCES AND NOTES

1. D. P. Schafer, E. K. Lehrman, A. G. Kautzman, R. Koyama, A. R. Mardinly, R. Yamasaki, R. M. Ransohoff, M. E. Greenberg, B. A. Barres, B. Stevens, Microglia sculpt postnatal neural circuits in an activity and complement-dependent manner. *Neuron* **74**, 691–705 (2012).
2. D. Fard, L. Tamagnone, Semaphorins in health and disease. *Cytokine Growth Factor Rev.* **57**, 55–63 (2021).
3. V. K. Ramanan, S. L. Risacher, K. Nho, S. Kim, L. Shen, B. C. McDonald, K. K. Yoder, G. D. Hutchins, J. D. West, E. F. Tallman, S. Gao, T. M. Foroud, M. R. Farlow, P. L. De Jager, D. A. Bennett, P. S. Aisen, R. C. Petersen, C. R. Jack, A. W. Toga, R. C. Green, W. J. Jagust, M. W. Weiner, A. J. Saykin, GWAS of longitudinal amyloid accumulation on ^{18}F-florbetapir PET in Alzheimer's disease implicates microglial activation gene *IL1RAP*. *Brain* **138**, 3076–3088 (2015).
4. C. S. McAlpine, J. Park, A. Griciuc, E. Kim, S. H. Choi, Y. Iwamoto, M. G. Kiss, K. A. Christie, C. Vinegoni, W. C. Poller, J. E. Mindur, C. T. Chan, S. He, H. Janssen, L. P. Wong, J. Downey, S. Singh, A. Anzai, F. Kahles, M. Jorfi, P. F. Feruglio, R. I. Sadreyev, R. Weissleder, B. P. Kleinstiver, M. Nahrendorf, R. E. Tanzi, F. K. Swirski, Astrocytic interleukin-3 programs microglia and limits Alzheimer's disease. *Nature* **595**, 701–706 (2021).
5. I. C. Clark, C. Gutiérrez-Vázquez, M. A. Wheeler, Z. Li, V. Rothhammer, M. Linnerbauer, L. M. Sanmarco, L. Guo, M. Blain, S. E. J. Zandee, C.-C. Chao, K. V. Batterman, M. Schwabenland, P. Lotfy, A. Tejeda-Velarde, P. Hewson, C. Manganeli Polonio, M. W. Shultis, Y. Salem, E. C. Tjon, P. H. Fonseca-Castro, D. M. Borucki, K. Alves de Lima, A. Plasencia, A. R. Abate, D. L. Rosene, K. J. Hodgetts, M. Prinz, J. P. Antel, A. Prat, F. J. Quintana, Barcoded viral tracing of single-cell interactions in central nervous system inflammation. *Science* **372**, eabf1230 (2021).
6. H. Lian, A. Litvinchuk, A. C.-A. Chiang, N. Aithmitti, J. L. Jankowsky, H. Zheng, Astrocyte-microglia cross talk through complement activation modulates amyloid pathology in mouse models of Alzheimer's disease. *J. Neurosci.* **36**, 577–589 (2016).
7. H. Yin, A. D. Flynn, Drugging membrane protein interactions. *Annu. Rev. Biomed. Eng.* **18**, 51–76 (2016).
8. J. P. Overington, B. Al-Lazikani, A. L. Hopkins, How many drug targets are there? *Nat. Rev. Drug Discov.* **5**, 993–996 (2006).
9. T. Worzfeld, S. Offermanns, Semaphorins and plexins as therapeutic targets. *Nat. Rev. Drug Discov.* **13**, 603–621 (2014).
10. J. C. Lambert, C. A. Ibrahim-Verbaas, D. Harold, A. C. Naj, R. Sims, C. Bellenguez, A. L. DeStafano, J. C. Bis, G. W. Beecham, B. Grenier-Boley, G. Russo, T. A. Thorton-Wells, N. Jones, A. V. Smith, V. Chouraki, C. Thomas, M. A. Ikram, D. Zelenika, B. N. Vardarajan, Y. Kamatani, C. F. Lin, A. Gerrish, H. Schmidt, B. Kunkle, M. L. Dunstan, A. Ruiz, M. T. Bihoreau, S. H. Choi, C. Reitz, F. Pasquier, C. Cruchaga, D. Craig, N. Amin, C. Berr, O. L. Lopez, P. L. De Jager, V. Deramecourt, J. A. Johnston, D. Evans, S. Lovestone, L. Letenneur, F. J. Morón, D. C. Rubinsztein, G. Eiriksdottir, K. Sleegers, A. M. Goate, N. Fiévet, M. W. Huentelman, M. Gill, K. Brown, M. I. Kamboh, L. Keller, P. Barberger-Gateau, B. McGuiness, E. B. Larson, R. Green, A. J. Myers, C. Dufouil, S. Todd, D. Wallon, S. Love, E. Rogaeva, J. Gallacher, P. S. George-Hyslop, J. Clarimon, A. Lleo, A. Bayer, D. W. Tsuang, L. Yu, M. Tsolaki, P. Bossù, G. Spalletta, P. Proitsi, J. Collinge, S. Sorbi, F. Sanchez-Garcia, N. C. Fox, J. Hardy, M. C. D. Naranjo, P. Bosco, R. Clarke, C. Brayne, D. Galimberti, M. Mancuso, F. Matthews, European Alzheimer's Disease Initiative (EADI), Genetic and Environmental Risk in Alzheimer's Disease, Alzheimer's Disease Genetic Consortium, Cohorts for Heart and Aging Research in Genomic Epidemiology, S. Moebus, P. Mecocci, M. Del Zompo, W. Maier, H. Hampel, A. Pilotto, M. Bullido, F. Panza, P. Caffarra, B. Nacmias, J. R. Gilbert, M. Mayhaus, L. Lannefelt, H. Hakonarson, S. Pichler, M. M. Carrasquillo, M. Ingelsson, D. Beekly, V. Alvarez, F. Zou, O. Valladares, S. G. Younkin, E. Coto, K. L. Hamilton-Nelson, W. Gu, C. Razquin, P. Pastor, I. Mateo, M. J. Owen, K. M. Faber, P. V. Jonsson, O. Combarros, M. C. O'Donovan, L. B. Cantwell, H. Soininen, D. Blacker, S. Mead, T. H. Mosley, D. A. Bennett, T. B. Harris, L. Fratiglioni, C. Holmes, R. F. de Bruijn, P. Passmore, T. J. Montine, K. Bettens, J. I. Rotter, A. Brice, K. Morgan, T. M. Foroud, W. A. Kukull, D. Hannequin, J. F. Powell, M. A. Nalls, K. Ritchie, K. L. Lunetta, J. S. Kauwe, E. Boerwinkle, M. Riemenschneider, M. Boada, M. Hiltuenen, E. R. Martin, R. Schmidt, D. Rujescu, L. S. Wang, J. F. Dartigues, R. Mayeux, C. Tzourio, A. Hofman, M. M. Nöthen, C. Graff, B. M. Psaty, L. Jones, J. L. Haines, P. A. Holmans, M. Lathrop, M. A. Pericak-Vance, L. J. Launer, L. A. Farrer, C. M. van Duijn, C. Van Broeckhoven,

V. Moskvina, S. Seshadri, J. Williams, G. D. Schellenberg, P. Amouyel, Meta-analysis of 74,046 individuals identifies 11 new susceptibility loci for Alzheimer's disease. *Nat. Genet.* **45**, 1452–1458 (2013).

11. B. W. Kunkle, B. Grenier-Boley, R. Sims, J. C. Bis, V. Damotte, A. C. Naj, A. Boland, M. Vronskaya, S. J. van der Lee, A. Amlie-Wolf, C. Bellenguez, A. Frizatti, V. Chouraki, E. R. Martin, K. Sleegers, N. Badarinarayan, J. Jakobsdottir, K. L. Hamilton-Nelson, S. Moreno-Grau, R. Olaso, R. Raybould, Y. Chen, A. B. Kuzma, M. Hiltunen, T. Morgan, S. Ahmad, B. N. Vardarajan, J. Epelbaum, P. Hoffmann, M. Boada, G. W. Beecham, J.-G. Garnier, D. Harold, A. L. Fitzpatrick, O. Valladares, M.-L. Moutet, A. Gerrish, A. V. Smith, L. Qu, D. Bacq, N. Denning, X. Jian, Y. Zhao, M. Del Zompo, N. C. Fox, S.-H. Choi, I. Mateo, J. T. Hughes, H. H. Adams, J. Malamon, F. Sanchez-Garcia, Y. Patel, J. A. Brody, B. A. Dombroski, M. C. D. Naranjo, M. Daniilidou, G. Eiriksdottir, S. Mukherjee, D. Wallon, J. Uphill, T. Aspelund, L. B. Cantwell, F. Garzia, D. Galimberti, E. Hofer, M. Butkiewicz, B. Fin, E. Scarpini, C. Sarnowski, W. S. Bush, S. Meslage, J. Kornhuber, C. C. White, Y. Song, R. C. Barber, S. Engelborghs, S. Sordon, D. Voijnovic, P. M. Adams, R. Vandenberghe, M. Mayhaus, L. A. Cupples, M. S. Albert, P. P. De Deyn, W. Gu, J. J. Himali, D. Beekly, A. Squassina, A. M. Hartmann, A. Orellana, D. Blacker, E. Rodriguez-Rodriguez, S. Lovestone, M. E. Garcia, R. S. Doody, C. Munoz-Fernadez, R. Sussams, H. Lin, T. J. Fairchild, Y. A. Benito, C. Holmes, H. Karamujić-Čomić, M. P. Frosch, H. Thonberg, W. Maier, G. Roshchupkin, B. Ghetti, V. Giedraitis, A. Kawalia, S. Li, R. M. Huebinger, L. Kilander, S. Moebus, I. Hernández, M. I. Kamboh, R. Brundin, J. Turton, Q. Yang, M. J. Katz, L. Concari, J. Lord, A. S. Beiser, C. D. Keene, S. Helisalmi, I. Kloszewska, W. A. Kukull, A. M. Koivisto, A. Lynch, L. Tarraga, E. B. Larson, A. Haapasalo, B. Lawlor, T. H. Mosley, R. B. Lipton, V. Solfrizzi, M. Gill, W. T. Longstreth, T. J. Montine, V. Frisardi, M. Diez-Fairen, F. Rivadeneira, R. C. Petersen, V. Deramecourt, I. Alvarez, F. Salani, A. Ciaramella, E. Boerwinkle, E. M. Reiman, N. Fievet, J. I. Rotter, J. S. Reisch, O. Hanon, C. Cupidi, A. G. A. Uitterlinden, D. R. Royall, C. Dufouil, R. G. Maletta, I. de Rojas, M. Sano, A. Brice, R. Cecchetti, P. S. George-Hyslop, K. Ritchie, M. Tsolaki, D. W. Tsuang, B. Dubois, D. Craig, C.-K. Wu, H. Soininen, D. Avramidou, R. L. Albin, L. Fratiglioni, A. Germanou, L. G. Apostolova, L. Keller, M. Koutroumani, S. E. Arnold, F. Panza, O. Gkatzima, S. Asthana, D. Hannequin, P. Whitehead, C. S. Atwood, P. Caffarra, H. Hampel, I. Quintela, Á. Carracedo, L. Lannfelt, D. C. Rubinsztein, L. L. Barnes, F. Pasquier, L. Frölich, S. Barral, B. McGuinness, T. G. Beach, J. A. Johnston, J. T. Becker, P. Passmore, E. H. Bigio, J. M. Schott, T. D. Bird, J. D. Warren, B. F. Boeve, M. K. Lupton, J. D. Bowen, P. Proitsi, A. Boxer, J. F. Powell, J. R. Burke, J. S. K. Kauwe, J. M. Burns, M. Mancuso, J. D. Buxbaum, U. Bonuccelli, N. J. Cairns, A. McQuillin, C. Cao, G. Livingston, C. S. Carlson, N. J. Bass, C. M. Carlsson, J. Hardy, R. M. Carney, J. Bras, M. M. Carrasquillo, R. Guerreiro, M. Allen, H. C. Chui, E. Fisher, C. Masullo, E. A. Crocco, C. DeCarli, G. Bisceglio, M. Dick, L. Ma, R. Duara, N. R. Graff-Radford, D. A. Evans, A. Hodges, K. M. Faber, M. Scherer, K. B. Fallon, M. Riemenschneider, D. W. Fardo, R. Heun, M. R. Farlow, H. Kölsch, S. Ferris, M. Leber, T. M. Foroud, I. Heuser, D. R. Galasko, I. Giegling, M. Gearing, M. Hüll, D. H. Geschwind, J. R. Gilbert, J. Morris, R. C. Green, K. Mayo, J. H. Growdon, T. Feulner, R. L. Hamilton, L. E. Harrell, D. Drichel, L. S. Honig, T. D. Cushion, M. J. Huentelman, P. Hollingworth, C. M. Hulette, B. T. Hyman, R. Marshall, G. P. Jarvik, A. Meggy, E. Abner, G. E. Menzies, L.-W. Jin, G. Leonenko, L. M. Real, G. R. Jun, C. T. Baldwin, D. Grozeva, A. Karydas, G. Russo, J. A. Kaye, R. Kim, F. Jessen, N. W. Kowall, B. Vellas, J. H. Kramer, E. Vardy, F. M. LaFerla, K.-H. Jöckel, J. J. Lah, M. Dichgans, J. B. Leverenz, D. Mann, A. I. Levey, S. Pickering-Brown, A. P. Lieberman, N. Klopp, K. L. Lunetta, H.-E. Wichmann, C. G. Lyketsos, K. Morgan, D. C. Marson, K. Brown, F. Martiniuk, C. Medway, D. C. Mash, M. M. Nöthen, E. Masliah, N. M. Hooper, W. C. McCormick, A. Daniele, S. M. McCurry, A. Bayer, A. N. McDavid, J. Gallacher, A. C. McKee, H. van den Bussche, M. Mesulam, C. Brayne, B. L. Miller, S. Riedel-Heller, C. A. Miller, J. W. Miller, A. Al-Chalabi, J. C. Morris, C. E. Shaw, A. J. Myers, J. Wiltfang, S. O'Bryant, J. M. Olichney, V. Alvarez, J. E. Parisi, A. B. Singleton, H. L. Paulson, J. Collinge, W. R. Perry, S. Mead, E. Peskind, D. H. Cribbs, M. Rossor, A. Pierce, N. S. Ryan, W. W. Poon, B. Nacmias, H. Potter, S. Sorbi, J. F. Quinn, E. Sacchinelli, A. Raj, G. Spalletta, M. Raskind, C. Caltagirone, P. Bossù, M. D. Orfei, B. Reisberg, R. Clarke, C. Reitz, A. D. Smith, J. M. Ringman, D. Warden, E. D. Roberson, G. Wilcock, E. Rogaeva, A. C. Bruni, H. J. Rosen, M. Gallo, R. N. Rosenberg, Y. Ben-Shlomo, M. A. Sager, P. Mecocci, A. J. Saykin, P. Pastor, M. L. Cuccaro, J. M. Vance, J. A. Schneider, L. S. Schneider, S. Slifer, W. W. Seeley, A. G. Smith, J. A. Sonnen, S. Spina, R. A. Stern, R. H. Swerdlow, M. Tang, R. E. Tanzi, J. Q. Trojanowski, J. C. Troncoso, V. M. Van Deerlin, L. J. Van Eldik, H. V. Vinters, J. P. Vonsattel, S. Weintraub, K. A. Welsh-Bohmer, K. C. Wilhelmsen, J. Williamson, T. S. Wingo, R. L. Woltjer, C. B. Wright, C.-E. Yu, L. Yu, Y. Saba, A. Pilotto, M. J. Bullido, O. Peters, P. K. Crane, D. Bennett, P. Bosco, E. Coto, V. Boccardi, P. L. De Jager, A. Lleo, N. Warner, O. L. Lopez, M. Ingelsson, P. Deloukas, C. Cruchaga, C. Graff, R. Gwilliam, M. Fornage, A. M. Goate, P. Sanchez-Juan, P. G. Kehoe, N. Amin, N. Ertekin-Taner, C. Berr, S. Debette, S. Love, L. J. Launer, S. G. Younkin, J.-F. Dartigues, C. Corcoran, M. A. Ikram, D. W. Dickson, G. Nicolas, D. Campion, J. Tschanz, H. Schmidt, H. Hakonarson, J. Clarimon, R. Munger, R. Schmidt, L. A. Farrer, C. Van Broeckhoven, M. C. O'Donovan, A. L. DeStefano, L. Jones, J. L. Haines, J.-F. Deleuze, M. J. Owen, V. Gudnason, R. Mayeux, V. Escott-Price, B. M. Psaty, A. Ramirez, L.-S. Wang, A. Ruiz, C. M. van Duijn, P. A. Holmans, S. Seshadri, J. Williams, P. Amouyel, G. D. Schellenberg, J.-C. Lambert, M. A. Pericak-Vance, Alzheimer Disease Genetics Consortium (ADGC), European Alzheimer's Disease Initiative (EADI), Cohorts for Heart and Aging Research in Genomic Epidemiology Consortium (CHARGE), Genetic and Environmental Risk in AD/Defining Genetic, Polygenic and Environmental Risk for Alzheimer's Disease Consortium (GERAD/PERADES), Genetic meta-analysis of diagnosed Alzheimer's disease identifies new risk loci and implicates Aβ, tau, immunity and lipid processing. *Nat. Genet.* **51**, 414–430 (2019).
12. J. Schwartzentruber, S. Cooper, J. Z. Liu, I. Barrio-Hernandez, E. Bello, N. Kumasaka, A. M. H. Young, R. J. M. Franklin, T. Johnson, K. Estrada, D. J. Gaffney, P. Beltrao, A. Bassett, Genome-wide meta-analysis, fine-mapping and integrative prioritization implicate new Alzheimer's disease risk genes. *Nat. Genet.* **53**, 392–402 (2021).
13. C. Bellenguez, F. Küçükali, I. E. Jansen, L. Kleineidam, S. Moreno-Grau, N. Amin, A. C. Naj, R. Campos-Martin, B. Grenier-Boley, V. Andrade, P. A. Holmans, A. Boland, V. Damotte, S. J. van der Lee, M. R. Costa, T. Kuulasmaa, Q. Yang, I. de Rojas, J. C. Bis, A. Yaqub, I. Prokic, J. Chapuis, S. Ahmad, V. Giedraitis, D. Aarsland, P. Garcia-Gonzalez, C. Abdelnour, E. Alarcón-Martín, D. Alcolea, M. Alegret, I. Alvarez, V. Álvarez, N. J. Armstrong, A. Tsolaki, C. Antúnez, I. Appollonio, M. Arcaro, S. Archetti, A. A. Pastor, B. Arosio, L. Athanasiu, H. Bailly, N. Banaj, M. Baquero, S. Barral, A. Beiser, A. B. Pastor, J. E. Below, P. Benchek, L. Benussi, C. Berr, C. Besse, V. Bessi, G. Binetti, A. Bizarro, R. Blesa, M. Boada, E. Boerwinkle, B. Borroni, S. Boschi, P. Bossù, G. Bråthen, J. Bressler, C. Bresner, H. Brodaty, K. J. Brookes, L. I. Brusco, D. Buiza-Rueda, K. Bûrger, V. Burholt, W. S. Bush, M. Calero, L. B. Cantwell, G. Chene, J. Chung, M. L. Cuccaro, Á. Carracedo, R. Cecchetti, L. Cervera-Carles, C. Charbonnier, H.-H. Chen, C. Chillotti, S. Ciccone, J. A. H. R. Claassen, C. Clark, E. Conti, A. Corma-Gómez, E. Costantini, C. Custodero, D. Daian, M. C. Dalmasso, A. Daniele, E. Dardiotis, J.-F. Dartigues, P. P. de Deyn, K. de Paiva Lopes, L. D. de Witte, S. Debette, J. Deckert, T. Del Ser, N. Denning, A. DeStefano, M. Dichgans, J. Diehl-Schmid, M. Diez-Fairen, P. D. Rossi, S. Djurovic, E. Duron, E. Düzel, C. Dufouil, G. Eiriksdottir, S. Engelborghs, V. Escott-Price, A. Espinosa, M. Ewers, K. M. Faber, T. Fabrizio, S. F. Nielsen, D. W. Fardo, L. Farotti, C. Fenoglio, M. Fernández-Fuertes, R. Ferrari, C. B. Ferreira, E. Ferri, B. Fin, P. Fischer, T. Fladby, K. Fließbach, B. Fongang, M. Fornage, J. Fortea, T. M. Foroud, S. Fostinelli, N. C. Fox, E. Franco-Macías, M. J. Bullido, A. Frank-García, L. Froelich, B. Fulton-Howard, D. Galimberti, J. M. García-Alberca, P. García-González, S. Garcia-Madrona, G. Garcia-Ribas, R. Ghidoni, I. Giegling, G. Giorgio, A. M. Goate, O. Goldhardt, D. Gomez-Fonseca, A. González-Pérez, C. Graff, G. Grande, E. Green, T. Grimmer, E. Grünblatt, M. Grunin, V. Gudnason, T. Guetta-Baranes, A. Haapasalo, G. Hadjigeorgiou, J. L. Haines, K. L. Hamilton-Nelson, H. Hampel, O. Hanon, J. Hardy, A. M. Hartmann, L. Hausner, J. Harwood, S. Heilmann-Heimbach, S. Helisalmi, M. T. Heneka, I. Hernández, M. J. Herrmann, P. Hoffmann, C. Holmes, H. Holstege, R. H. Vilas, M. Hulsman, J. Humphrey, G. J. Biessels, X. Jian, C. Johansson, G. R. Jun, Y. Kastumata, J. Kauwe, P. G. Kehoe, L. Kilander, A. K. Ståhlbom, M. Kivipelto, A. Koivisto, J. Kornhuber, M. H. Kosmidis, W. A. Kukull, P. P. Kuksa, B. W. Kunkle, A. B. Kuzma, C. Lage, E. J. Laukka, L. Launer, A. Lauria, C.-Y. Lee, J. Lehtisalo, O. Lerch, A. Lleó, W. Longstreth, O. Lopez, A. L. de Munain, S. Love, M. Löwemark, L. Luckcuck, K. L. Lunetta, Y. Ma, J. Macías, C. A. MacLeod, W. Maier, F. Mangialasche, M. Spallazzi, M. Marquié, R. Marshall, E. R. Martin, A. M. Montes, C. M. Rodríguez, C. Masullo, R. Mayeux, S. Mead, P. Mecocci, M. Medina, A. Meggy, S. Mehrabian, S. Mendoza, M. Menéndez-González, P. Mir, S. Moebus, M. Mol, L. Molina-Porcel, L. Montrreal, L. Morelli, F. Moreno, K. Morgan, T. Mosley, M. M. Nöthen, C. Muchnik, S. Mukherjee, B. Nacmias, T. Ngandu, G. Nicolas, B. G. Nordestgaard, R. Olaso, A. Orellana, M. Orsini, G. Ortega, A. Padovani, C. Paolo, G. Papenberg, L. Parnetti, F. Pasquier, P. Pastor, G. Peloso, A. Pérez-Cordón, J. Pérez-Tur, P. Pericard, O. Peters, Y. A. L. Pijnenburg, J. A. Pineda, G. Piñol-Ripoll, C. Pisanu, T. Polak, J. Popp, D. Posthuma, J. Priller, R. Puerta, O. Quenez, I. Quintela, J. Q. Thomassen, A. Rábano, I. Rainero, F. Rajabli, I. Ramakers, L. M. Real, M. J. T. Reinders, C. Reitz, D. Reyes-Dumeyer, P. Ridge, S. Riedel-Heller, P. Riederer, N. Roberto, E. Rodriguez-Rodriguez, A. Rongve, I. R. Allende, M. Rosende-Roca, J. L. Royo, E. Rubino, D. Rujescu, M. E. Sáez, P. Sakka, I. Saltvedt, Á. Sanabria, M. B. Sánchez-Arjona, F. Sanchez-Garcia, P. S. Juan, R. Sánchez-Valle, S. B. Sando, C. Sarnowski, C. L. Satizabal, M. Scamosci, N. Scarmeas, E. Scarpini, P. Scheltens, N. Scherbaum, M. Scherer, M. Schmid, A. Schneider, J. M. Schott, G. Selbæk, D. Seripa, M. Serrano, J. Sha, A. A. Shadrin, O. Skrobot, S. Slifer, G. J. L. Snijders, H. Soininen, V. Solfrizzi, A. Solomon, Y. Song, S. Sorbi, O. Sotolongo-Grau, G. Spalletta, A. Spottke, A. Squassina, E. Stordal, J. P. Tartan, L. Tárraga, N. Tesí, A. Thalamuthu, T. Thomas, G. Tosto, L. Traykov, L. Tremolizzo, A. Tybjærg-Hansen, A. Uitterlinden, A. Ullgren, I. Ulstein, S. Valero, O. Valladares, C. V. Broeckhoven, J. Vance, B. N. Vardarajan, A. van der Lugt, J. V. Dongen, J. van Rooij, J. van Swieten, R. Vandenberghe, F. Verhey, J.-S. Vidal, J. Vogelgsang, M. Vyhnalek, M. Wagner, D. Wallon, L.-S. Wang, R. Wang, L. Weinhold, J. Wiltfang, G. Windle, B. Woods, M. Yannakoulia, H. Zare, Y. Zhao, X. Zhang, C. Zhu, M. Zulaica, EADB, GR@ACE, DEGESCO, EADI, GERAD, Demgene, FinnGen, ADGC, CHARGE, L. A. Farrer, B. M. Psaty, M. Ghanbari, T. Raj, P. Sachdev, K. Mather, F. Jessen, M. A. Ikram, A. de Mendonça, J. Hort, M. Tsolaki, M. A. Pericak-Vance, P. Amouyel, J. Williams, R. Frikke-Schmidt, J. Clarimon, J.-F. Deleuze, G. Rossi, S. Seshadri, O. A. Andreassen, M. Ingelsson, M. Hiltunen, K. Sleegers, G. D. Schellenberg, C. M. van Duijn, R. Sims, W. M. van der Flier, A. Ruiz, A. Ramirez, J.-C. Lambert, New insights into the genetic etiology of Alzheimer's disease and related dementias. *Nat. Genet.* **54**, 412–436 (2022).

14. L. Brase, S.-F. You, R. D'Oliveira Albanus, J. L. Del-Aguila, Y. Dai, B. C. Novotny, C. Soriano-Tarraga, T. Dykstra, M. V. Fernandez, J. P. Budde, K. Bergmann, J. C. Morris, R. J. Bateman, R. J. Perrin, E. McDade, C. Xiong, A. M. Goate, M. Farlow, Dominantly Inherited Alzheimer Network (DIAN), G. T. Sutherland, J. Kipnis, C. M. Karch, B. A. Benitez, O. Harari, Single-nucleus RNA-sequencing of autosomal dominant Alzheimer disease and risk variant carriers. *Nat. Commun.* **14**, 2314 (2023).
15. M. Olah, V. Menon, N. Habib, M. F. Taga, Y. Ma, C. J. Yung, M. Cimpean, A. Khairallah, G. Coronas-Samano, R. Sankowski, D. Grün, A. A. Kroshilina, D. Dionne, R. A. Sarkis, G. R. Cosgrove, J. Helgager, J. A. Golden, P. B. Pennell, M. Prinz, J. P. G. Vonsattel, A. F. Teich, J. A. Schneider, D. A. Bennett, A. Regev, W. Elyaman, E. M. Bradshaw, P. L. De Jager, Single cell RNA sequencing of human microglia uncovers a subset associated with Alzheimer's disease. *Nat. Commun.* **11**, 6129 (2020).
16. S.-F. Lau, H. Cao, A. K. Y. Fu, N. Y. Ip, Single-nucleus transcriptome analysis reveals dysregulation of angiogenic endothelial cells and neuroprotective glia in Alzheimer's disease. *Proc. Natl. Acad. Sci. U.S.A.* **117**, 25800–25809 (2020).
17. S. Morabito, E. Miyoshi, N. Michael, S. Shahin, A. C. Martini, E. Head, J. Silva, K. Leavy, M. Perez-Rosendahl, V. Swarup, Single-nucleus chromatin accessibility and transcriptomic characterization of Alzheimer's disease. *Nat. Genet.* **53**, 1143–1155 (2021).
18. N. M. Dräger, S. M. Sattler, C. T.-L. Huang, O. M. Teter, K. Leng, S. H. Hashemi, J. Hong, C. D. Clelland, L. Zhan, L. Kodama, A. B. Singleton, M. A. Nalls, J. Ichida, M. E. Ward, F. Faghri, L. Gan, M. Kampmann, A CRISPRi/a platform in human iPSC-derived microglia uncovers regulators of disease states. *Nat. Neurosci.* **25**, 1149–1162 (2022).
19. Q. Li, B. A. Barres, Microglia and macrophages in brain homeostasis and disease. *Nat. Rev. Immunol.* **18**, 225–242 (2018).
20. M. Efremova, M. Vento-Tormo, S. A. Teichmann, R. Vento-Tormo, CellPhoneDB: Inferring cell–cell communication from combined expression of multi-subunit ligand–receptor complexes. *Nat. Protoc.* **15**, 1484–1506 (2020).
21. P. J. Paasila, D. S. Davies, J. J. Kril, C. Goldsbury, G. T. Sutherland, The relationship between the morphological subtypes of microglia and Alzheimer's disease neuropathology. *Brain Pathol.* **29**, 726–740 (2019).
22. Y. Zhou, W. M. Song, P. S. Andhey, A. Swain, T. Levy, K. R. Miller, P. L. Poliani, M. Cominelli, S. Grover, S. Gilfillan, M. Cella, T. K. Ulland, K. Zaitsev, A. Miyashita, T. Ikeuchi, M. Sainouchi, A. Kakita, D. A. Bennett, J. A. Schneider, M. R. Nichols, S. A. Beausoleil, J. D. Ulrich, D. M. Holtzman, M. N. Artyomov, M. Colonna, Human and mouse single-nucleus transcriptomics reveal TREM2-dependent and TREM2-independent cellular responses in Alzheimer's disease. *Nat. Med.* **26**, 131–142 (2020).
23. S. B. Taylor, J. A. Markham, A. R. Taylor, B. Z. Kanaskie, J. I. Koenig, Sex-specific neuroendocrine and behavioral phenotypes in hypomorphic type II Neuregulin 1 rats. *Behav. Brain Res.* **224**, 223–232 (2011).
24. I. E. Jansen, J. E. Savage, K. Watanabe, J. Bryois, D. M. Williams, S. Steinberg, J. Sealock, I. K. Karlsson, S. Hägg, L. Athanasiu, N. Voyle, P. Proitsi, A. Witoelar, S. Stringer, D. Aarsland, I. S. Almdahl, F. Andersen, S. Bergh, F. Bettella, S. Bjornsson, A. Brækhus, G. Bråthen, C. de Leeuw, R. S. Desikan, S. Djurovic, L. Dumitrescu, T. Fladby, T. J. Hohman, P. V. Jonsson, S. J. Kiddle, A. Rongve, I. Saltvedt, S. B. Sando, G. Selbæk, M. Shoai, N. G. Skene, J. Snaedal, E. Stordal, I. D. Ulstein, Y. Wang, L. R. White, J. Hardy, J. Hjerling-Leffler, P. F. Sullivan, W. M. van der Flier, R. Dobson, L. K. Davis, H. Stefansson, K. Stefansson, N. L. Pedersen, S. Ripke, O. A. Andreassen, D. Posthuma, Genome-wide meta-analysis identifies new loci and functional pathways influencing Alzheimer's disease risk. *Nat. Genet.* **51**, 404–413 (2019).
25. R. E. Marioni, S. E. Harris, Q. Zhang, A. F. McRae, S. P. Hagenaars, W. D. Hill, G. Davies, C. W. Ritchie, C. R. Gale, J. M. Starr, A. M. Goate, D. J. Porteous, J. Yang, K. L. Evans, I. J. Deary, N. R. Wray, P. M. Visscher, GWAS on family history of Alzheimer's disease. *Transl. Psychiatry* **8**, 99 (2018).
26. Y. Deming, F. Filipello, F. Cignarella, C. Cantoni, S. Hsu, R. Mikesell, Z. Li, J. L. Del-Aguila, U. Dube, F. G. Farias, J. Bradley, J. Budde, L. Ibanez, M. V. Fernandez, K. Blennow, H. Zetterberg, A. Heslegrave, P. M. Johansson, J. Svensson, B. Nellgård, A. Lleo, D. Alcolea, J. Clarimon, L. Rami, J. L. Molinuevo, M. Suárez-Calvet, E. Morenas-Rodríguez, G. Kleinberger, M. Ewers, O. Harari, C. Haass, T. J. Brett, B. A. Benitez, C. M. Karch, L. Piccio, C. Cruchaga, The MS4A gene cluster is a key modulator of soluble TREM2 and Alzheimer's disease risk. *Sci. Transl. Med.* **11**, eaau2291 (2019).
27. Y. Hu, T. Peng, L. Gao, K. Tan, CytoTalk: De novo construction of signal transduction networks using single-cell transcriptomic data. *Sci. Adv.* **7**, eabf1356 (2021).
28. Z. Szepesi, O. Manouchehrian, S. Bachiller, T. Deierborg, Bidirectional microglia-neuron communication in health and disease. *Front. Cell. Neurosci.* **12**, 323 (2018).
29. N. Takegahara, H. Takamatsu, T. Toyofuku, T. Tsujimura, T. Okuno, K. Yukawa, M. Mizui, M. Yamamoto, D. V. R. Prasad, K. Suzuki, M. Ishii, K. Terai, M. Moriya, Y. Nakatsuji, S. Sakoda, S. Sato, S. Akira, K. Takeda, M. Inui, T. Takai, M. Ikawa, M. Okabe, A. Kumanogoh, H. Kikutani, Plexin-A1 and its interaction with DAP12 in immune responses and bone homeostasis. *Nat. Cell Biol.* **8**, 615–622 (2006).
30. N. Thrupp, C. Sala Frigerio, L. Wolfs, N. G. Skene, N. Fattorelli, S. Poovathingal, Y. Fourne, P. M. Matthews, T. Theys, R. Mancuso, B. de Strooper, M. Fiers, Single-nucleus RNA-seq is not suitable for detection of microglial activation genes in humans. *Cell Rep.* **32**, 108189 (2020).
31. X. Wang, Y. He, Q. Zhang, X. Ren, Z. Zhang, Direct comparative analyses of 10X genomics chromium and smart-seq2. *Genomics Proteomics Bioinformatics* **19**, 253–266 (2021).
32. T. K. Ulland, M. Colonna, TREM2 - A key player in microglial biology and Alzheimer disease. *Nat. Rev. Neurol.* **14**, 667–675 (2018).
33. Y. Atagi, C.-C. Liu, M. M. Painter, X.-F. Chen, C. Verbeeck, H. Zheng, X. Li, R. Rademakers, S. S. Kang, H. Xu, S. Younkin, P. Das, J. D. Fryer, G. Bu, Apolipoprotein E is a ligand for triggering receptor expressed on myeloid cells 2 (TREM2). *J. Biol. Chem.* **290**, 26043–26050 (2015).
34. F. L. Yeh, Y. Wang, I. Tom, L. C. Gonzalez, M. Sheng, TREM2 binds to apolipoproteins, including APOE and CLU/APOJ, and thereby facilitates uptake of amyloid-beta by microglia. *Neuron* **91**, 328–340 (2016).
35. S. M. Neuner, J. Tcw, A. M. Goate, Genetic architecture of Alzheimer's disease. *Neurobiol. Dis.* **143**, 104976 (2020).
36. E. Rogaeva, Y. Meng, J. H. Lee, Y. Gu, T. Kawarai, F. Zou, T. Katayama, C. T. Baldwin, R. Cheng, H. Hasegawa, F. Chen, N. Shibata, K. L. Lunetta, R. Pardossi-Piquard, C. Bohm, Y. Wakutani, L. A. Cupples, K. T. Cuenco, R. C. Green, L. Pinessi, I. Rainero, S. Sorbi, A. Bruni, R. Duara, R. P. Friedland, R. Inzelberg, W. Hampe, H. Bujo, Y.-Q. Song, O. M. Andersen, T. E. Willnow, N. Graff-Radford, R. C. Petersen, D. Dickson, S. D. Der, P. E. Fraser, G. Schmitt-Ulms, S. Younkin, R. Mayeux, L. A. Farrer, P. St George-Hyslop, The neuronal sortilin-related receptor SORL1 is genetically associated with Alzheimer disease. *Nat. Genet.* **39**, 168–177 (2007).
37. R.-H. Yin, J.-T. Yu, L. Tan, The role of SORL1 in Alzheimer's disease. *Mol. Neurobiol.* **51**, 909–918 (2015).
38. S. Chen, Y. Chang, L. Li, D. Acosta, Y. Li, Q. Guo, C. Wang, E. Turkes, C. Morrison, D. Julian, M. E. Hester, D. W. Scharre, C. Santiskulvong, S. X. Song, J. T. Plummer, G. E. Serrano, T. G. Beach, K. E. Duff, Q. Ma, H. Fu, Spatially resolved transcriptomics reveals genes associated with the vulnerability of middle temporal gyrus in Alzheimer's disease. *Acta Neuropathol. Commun.* **10**, 188 (2022).
39. H. Keren-Shaul, A. Spinrad, A. Weiner, O. Matcovitch-Natan, R. Dvir-Szternfeld, T. K. Ulland, E. David, K. Baruch, D. Lara-Astaiso, B. Toth, S. Itzkovitz, M. Colonna, M. Schwartz, I. Amit, A unique microglia type associated with restricting development of Alzheimer's disease. *Cell* **169**, 1276–1290.e17 (2017).
40. A. McQuade, M. Coburn, C. H. Tu, J. Hasselmann, H. Davtyan, M. Blurton-Jones, Development and validation of a simplified method to generate human microglia from pluripotent stem cells. *Mol. Neurodegener.* **13**, 67 (2018).
41. W.-Y. Wang, M.-S. Tan, J.-T. Yu, L. Tan, Role of pro-inflammatory cytokines released from microglia in Alzheimer's disease. *Ann. Transl. Med.* **3**, 136 (2015).
42. A. Grubman, X. Y. Choo, G. Chew, J. F. Ouyang, G. Sun, N. P. Croft, F. J. Rossello, R. Simmons, S. Buckberry, D. V. Landin, J. Pflueger, T. H. Vandekolk, Z. Abay, Y. Zhou, X. Liu, J. Chen, M. Larcombe, J. M. Haynes, C. McLean, S. Williams, S. Y. Chai, T. Wilson, R. Lister, C. W. Pouton, A. W. Purcell, O. J. L. Rackham, E. Petretto, J. M. Polo, Transcriptional signature in microglia associated with Aβ plaque phagocytosis. *Nat. Commun.* **12**, 3015 (2021).
43. S. Safaiyan, S. Besson-Girard, T. Kaya, L. Cantuti-Castelvetri, L. Liu, H. Ji, M. Schifferer, G. Gouna, F. Usifo, N. Kannaiyan, D. Fitzner, X. Xiang, M. J. Rossner, M. Brendel, O. Gokce, M. Simons, White matter aging drives microglial diversity. *Neuron* **109**, 1100–1117.e10 (2021).
44. T. R. Jay, V. E. von Saucken, G. E. Landreth, TREM2 in neurodegenerative diseases. *Mol. Neurodegener.* **12**, 56 (2017).
45. A. McQuade, Y. J. Kang, J. Hasselmann, A. Jairaman, A. Sotelo, M. Coburn, S. K. Shabestari, J. P. Chadarevian, G. Fote, C. H. Tu, E. Danhash, J. Silva, E. Martinez, C. Cotman, G. A. Prieto, L. M. Thompson, J. S. Steffan, I. Smith, H. Davtyan, M. Cahalan, H. Cho, M. Blurton-Jones, Gene expression and functional deficits underlie TREM2-knockout microglia responses in human models of Alzheimer's disease. *Nat. Commun.* **11**, 5370 (2020).
46. J. Park, I. Wetzel, I. Marriott, D. Dréau, C. D'Avanzo, D. Y. Kim, R. E. Tanzi, H. Cho, A 3D human triculture system modeling neurodegeneration and neuroinflammation in Alzheimer's disease. *Nat. Neurosci.* **21**, 941–951 (2018).
47. S. S. Kwak, K. J. Washicosky, E. Brand, D. von Maydell, J. Aronson, S. Kim, D. E. Capen, M. Cetinbas, R. Sadreyev, S. Ning, E. Bylykbashi, W. Xia, S. L. Wagner, S. H. Choi, R. E. Tanzi, D. Y. Kim, Amyloid-β42/40 ratio drives tau pathology in 3D human neural cell culture models of Alzheimer's disease. *Nat. Commun.* **11**, 1377 (2020).
48. P. Naderi Yeganeh, S. S. Kwak, M. Jorfi, K. Koler, T. Kalatturu, D. von Maydell, Z. Liu, K. Guo, Y. Choi, J. Park, N. Abarca, G. Bakiasi, M. Cetinbas, R. Sadreyev, A. Griciuc, L. Quinti, S. H. Choi, W. Xia, R. E. Tanzi, W. Hide, D. Y. Kim, Integrative pathway analysis across humans and 3D cellular models identifies the p38 MAPK-MK2 axis as a therapeutic target for Alzheimer's disease. *Neuron* **113**, 205–224.e8 (2025).
49. H. Mathys, Z. Peng, C. A. Boix, M. B. Victor, N. Leary, S. Babu, G. Abdelhady, X. Jiang, A. P. Ng, K. Ghafari, A. K. Kunisky, J. Mantero, K. Galani, V. N. Lohia, G. E. Fortier, Y. Lotfi, J. Ivey, H. P. Brown, P. R. Patel, N. Chakraborty, J. I. Beaudway, E. J. Imhoff, C. F. Keeler, M. M. McChesney, H. H. Patel, S. P. Patel, M. T. Thai, D. A. Bennett, M. Kellis, L.-H. Tsai,

Single-cell atlas reveals correlates of high cognitive function, dementia, and resilience to Alzheimer's disease pathology. *Cell* **186**, 4365–4385.e27 (2023).
50. M. I. Gabitto, K. J. Travaglini, V. M. Rachleff, E. S. Kaplan, B. Long, J. Ariza, Y. Ding, J. T. Mahoney, N. Dee, J. Goldy, E. J. Melief, A. Agrawal, O. Kana, X. Zhen, S. T. Barlow, K. Brouner, J. Campos, J. Campos, A. J. Carr, T. Casper, R. Chakrabarty, M. Clark, J. Cool, R. Dalley, M. Darvas, S.-L. Ding, T. Dolbeare, T. Egdorf, L. Esposito, R. Ferrer, L. E. Fleckenstein, R. Gala, A. Gary, E. Gelfand, J. Gloe, N. Guilford, J. Guzman, D. Hirschstein, W. Ho, M. Hupp, T. Jarsky, N. Johansen, B. E. Kalmbach, L. M. Keene, S. Khawand, M. D. Kilgore, A. Kirkland, M. Kunst, B. R. Lee, M. Leytze, C. L. M. Donald, J. Malone, Z. Maltzer, N. Martin, R. McCue, D. McMillen, G. Mena, E. Meyerdierks, K. P. Meyers, T. Mollenkopf, M. Montine, A. L. Nolan, J. K. Nyhus, P. A. Olsen, M. Pacleb, C. M. Pagan, N. Peña, T. Pham, C. A. Pom, N. Postupna, C. Rimorin, A. Ruiz, G. A. Saldi, A. M. Schantz, N. V. Shapovalova, S. A. Sorensen, B. Staats, M. Sullivan, S. M. Sunkin, C. Thompson, M. Tieu, J. T. Ting, A. Torkelson, T. Tran, N. J. V. Cuevas, S. Walling-Bell, M.-Q. Wang, J. Waters, A. M. Wilson, M. Xiao, D. Haynor, N. M. Gatto, S. Jayadev, S. Mufti, L. Ng, S. Mukherjee, P. K. Crane, C. S. Latimer, B. P. Levi, K. A. Smith, J. L. Close, J. A. Miller, R. D. Hodge, E. B. Larson, T. J. Grabowski, M. Hawrylycz, C. D. Keene, E. S. Lein, Integrated multimodal cell atlas of Alzheimer's disease. *Nat. Neurosci.* **27**, 2366–2383 (2024).
51. G. Jun, H. Asai, E. Zeldich, E. Drapeau, C. Chen, J. Chung, J.-H. Park, S. Kim, V. Haroutunian, T. Foroud, R. Kuwano, J. L. Haines, M. A. Pericak-Vance, G. D. Schellenberg, K. L. Lunetta, J.-W. Kim, J. D. Buxbaum, R. Mayeux, T. Ikezu, C. R. Abraham, L. A. Farrer, PLXNA4 is associated with Alzheimer disease and modulates tau phosphorylation. *Ann. Neurol.* **76**, 379–392 (2014).
52. P. F. Good, D. Alapat, A. Hsu, C. Chu, D. Perl, X. Wen, D. E. Burstein, D. S. Kohtz, A role for semaphorin 3A signaling in the degeneration of hippocampal neurons during Alzheimer's disease. *J. Neurochem.* **91**, 716–736 (2004).
53. F. Nakamura, R. G. Kalb, S. M. Strittmatter, Molecular basis of semaphorin-mediated axon guidance. *J. Neurobiol.* **44**, 219–229 (2000).
54. A. Kumanogoh, H. Kikutani, Immunological functions of the neuropilins and plexins as receptors for semaphorins. *Nat. Rev. Immunol.* **13**, 802–814 (2013).
55. S. S. Kang, A. Kurti, A. Wojtas, K. E. Baker, C.-C. Liu, T. Kanekiyo, Y. Deming, C. Cruchaga, S. Estus, G. Bu, J. D. Fryer, Identification of plexin A4 as a novel clusterin receptor links two Alzheimer's disease risk genes. *Hum. Mol. Genet.* **25**, 3467–3475 (2016).
56. E. E. Evans, V. Mishra, C. Mallow, E. M. Gersz, L. Balch, A. Howell, C. Reilly, E. S. Smith, T. L. Fisher, M. Zauderer, Semaphorin 4D is upregulated in neurons of diseased brains and triggers astrocyte reactivity. *J. Neuroinflammation* **19**, 200 (2022).
57. T. Ito, K. Yoshida, T. Negishi, M. Miyajima, H. Takamatsu, H. Kikutani, A. Kumanogoh, K. Yukawa, Plexin-A1 is required for Toll-like receptor-mediated microglial activation in the development of lipopolysaccharide-induced encephalopathy. *Int. J. Mol. Med.* **33**, 1122–1130 (2014).
58. J. Klesney-Tait, I. R. Turnbull, M. Colonna, The TREM receptor family and signal integration. *Nat. Immunol.* **7**, 1266–1273 (2006).
59. D. L. Kober, T. J. Brett, TREM2-Ligand interactions in health and disease. *J. Mol. Biol.* **429**, 1607–1629 (2017).
60. S. Chung, J. Yang, H. J. Kim, E. M. Hwang, W. Lee, K. Suh, H. Choi, I. Mook-Jung, Plexin-A4 mediates amyloid-β-induced tau pathology in Alzheimer's disease animal model. *Prog. Neurobiol.* **203**, 102075 (2021).
61. S. Kang, Y. Nakanishi, Y. Kioi, D. Okuzaki, T. Kimura, H. Takamatsu, S. Koyama, S. Nojima, M. Nishide, Y. Hayama, Y. Kinehara, Y. Kato, T. Nakatani, T. Shimogori, J. Takagi, T. Toyofuku, A. Kumanogoh, Semaphorin 6D reverse signaling controls macrophage lipid metabolism and anti-inflammatory polarization. *Nat. Immunol.* **19**, 561–570 (2018).
62. A. Millet, J. H. Ledo, S. F. Tavazoie, An exhausted-like microglial population accumulates in aged and APOE4 genotype Alzheimer's brains. *Immunity* **57**, 153–170.e6 (2024).
63. Q. Han, Y.-A. Sun, Y. Zong, C. Chen, H.-F. Wang, L. Tan, Alzheimer's Disease Neuroimaging Initiative, Common variants in *PLXNA4* and correlation to CSF-related phenotypes in Alzheimer's disease. *Front. Neurosci.* **12**, 946 (2018).
64. A. Macedo, C. Gómez, M. Â. Rebelo, J. Poza, I. Gomes, S. Martins, A. Maturana-Candelas, V. G. Pablo, L. Durães, P. Sousa, M. Figueruelo, M. Rodríguez, C. Pita, M. Arenas, L. Álvarez, R. Hornero, A. M. Lopes, N. Pinto, Risk variants in three Alzheimer's disease genes show association with EEG endophenotypes. *J. Alzheimers Dis.* **80**, 209–223 (2021).
65. Y. Deming, Z. Li, M. Kapoor, O. Harari, J. L. Del-Aguila, K. Black, D. Carrell, Y. Cai, M. V. Fernandez, J. Budde, S. Ma, B. Saef, B. Howells, K.-L. Huang, S. Bertelsen, A. M. Fagan, D. M. Holtzman, J. C. Morris, S. Kim, A. J. Saykin, P. L. De Jager, M. Albert, A. Moghekar, R. O'Brien, M. Riemenschneider, R. C. Petersen, K. Blennow, H. Zetterberg, L. Minthon, V. M. Van Deerlin, V. M.-Y. Lee, L. M. Shaw, J. Q. Trojanowski, G. Schellenberg, J. L. Haines, R. Mayeux, M. A. Pericak-Vance, L. A. Farrer, E. R. Peskind, G. Li, A. F. Di Narzo, Alzheimer's Disease Neuroimaging Initiative (ADNI), Alzheimer Disease Genetic Consortium (ADGC), J. S. K. Kauwe, A. M. Goate, C. Cruchaga, Genome-wide association study identifies four novel loci associated with Alzheimer's endophenotypes and disease modifiers. *Acta Neuropathol.* **133**, 839–856 (2017).
66. A. Zettergren, K. Höglund, S. Kern, V. Thorvaldsson, M. Johan Skoog, O. Hansson, N. Andreasen, N. Bogdanovic, K. Blennow, I. Skoog, H. Zetterberg, Association of IL1RAP-related genetic variation with cerebrospinal fluid concentration of Alzheimer-associated tau protein. *Sci. Rep.* **9**, 2460 (2019).
67. F. Su, F. Bai, Z. Zhang, Inflammatory cytokines and Alzheimer's disease: A review from the perspective of genetic polymorphisms. *Neurosci. Bull.* **32**, 469–480 (2016).
68. G. Ogunmokun, S. Dewanjee, P. Chakraborty, C. Valupadas, A. Chaudhary, V. Kolli, U. Anand, J. Vallamkondu, P. Goel, H. P. R. Paluru, K. D. Gill, P. H. Reddy, V. De Feo, R. Kandimalla, The potential role of cytokines and growth factors in the pathogenesis of Alzheimer's disease. *Cells* **10**, 2790 (2021).
69. A. S. Mendiola, A. E. Cardona, The IL-1β phenomena in neuroinflammatory diseases. *J. Neural Transm. (Vienna)* **125**, 781–795 (2018).
70. H. Mathys, J. Davila-Velderrain, Z. Peng, F. Gao, S. Mohammadi, J. Z. Young, M. Menon, L. He, F. Abdurrob, X. Jiang, A. J. Martorell, R. M. Ransohoff, B. P. Hafler, D. A. Bennett, M. Kellis, L.-H. Tsai, Single-cell transcriptomic analysis of Alzheimer's disease. *Nature* **570**, 332–337 (2019).
71. T. Stuart, A. Butler, P. Hoffman, C. Hafemeister, E. Papalexi, W. M. Mauck, Y. Hao, M. Stoeckius, P. Smibert, R. Satija, Comprehensive integration of single-cell data. *Cell* **177**, 1888–1902.e21 (2019).
72. J. L. Del-Aguila, Z. Li, U. Dube, K. A. Mihindukulasuriya, J. P. Budde, M. V. Fernandez, L. Ibanez, J. Bradley, F. Wang, K. Bergmann, R. Davenport, J. C. Morris, D. M. Holtzman, R. J. Perrin, B. A. Benitez, J. Dougherty, C. Cruchaga, O. Harari, A single-nuclei RNA sequencing study of mendelian and sporadic AD in the human brain. *Alzheimers Res. Ther.* **11**, 71 (2019).
73. T. Kamath, A. Abdulraouf, S. J. Burris, J. Langlieb, V. Gazestani, N. M. Nadaf, K. Balderrama, C. Vanderburg, E. Z. Macosko, Single-cell genomic profiling of human dopamine neurons identifies a population that selectively degenerates in Parkinson's disease. *Nat. Neurosci.* **25**, 588–595 (2022).
74. C. Hafemeister, R. Satija, Normalization and variance stabilization of single-cell RNA-seq data using regularized negative binomial regression. *Genome Biol.* **20**, 296 (2019).
75. Y. Zhang, T. Liu, C. A. Meyer, J. Eeckhoute, D. S. Johnson, B. E. Bernstein, C. Nussbaum, R. M. Myers, M. Brown, W. Li, X. S. Liu, Model-based analysis of ChIP-seq (MACS). *Genome Biol.* **9**, R137 (2008).
76. H. M. Amemiya, A. Kundaje, A. P. Boyle, The ENCODE blacklist: Identification of problematic regions of the genome. *Sci. Rep.* **9**, 9354 (2019).
77. H. A. Pliner, J. S. Packer, J. L. McFaline-Figueroa, D. A. Cusanovich, R. M. Daza, D. Aghamirzaie, S. Srivatsan, X. Qiu, D. Jackson, A. Minkina, A. C. Adey, F. J. Steemers, J. Shendure, C. Trapnell, Cicero predicts cis-regulatory DNA interactions from single-cell chromatin accessibility data. *Mol. Cell* **71**, 858–871.e8 (2018).
78. S. Yang, S. E. Corbett, Y. Koga, Z. Wang, W. E. Johnson, M. Yajima, J. D. Campbell, Decontamination of ambient RNA in single-cell RNA-seq with DecontX. *Genome Biol.* **21**, 57 (2020).
79. D. Szklarczyk, A. L. Gable, K. C. Nastou, D. Lyon, R. Kirsch, S. Pyysalo, N. T. Doncheva, M. Legeay, T. Fang, P. Bork, L. J. Jensen, C. von Mering, The STRING database in 2021: Customizable protein-protein networks, and functional characterization of user-uploaded gene/measurement sets. *Nucleic Acids Res.* **49**, D605–D612 (2021).
80. P. Shannon, A. Markiel, O. Ozier, N. S. Baliga, J. T. Wang, D. Ramage, N. Amin, B. Schwikowski, T. Ideker, Cytoscape: A software environment for integrated models of biomolecular interaction networks. *Genome Res.* **13**, 2498–2504 (2003).
81. J. A. Gustavsen, S. Pai, R. Isserlin, B. Demchak, A. R. Pico, RCy3: Network biology using Cytoscape from within R. *F1000Res* **8**, 1774 (2019).
82. J. H. Morris, L. Apeltsin, A. M. Newman, J. Baumbach, T. Wittkop, G. Su, G. D. Bader, T. E. Ferrin, clusterMaker: A multi-algorithm clustering plugin for Cytoscape. *BMC Bioinformatics* **12**, 436 (2011).
83. C. E. Shannon, A mathematical theory of communication. *Bell Syst. Tech. J.* **27**, 379–423 (1948).
84. A. A. Margolin, I. Nemenman, K. Basso, C. Wiggins, G. Stolovitzky, R. Dalla Favera, A. Califano, ARACNE: An algorithm for the reconstruction of gene regulatory networks in a mammalian cellular context. *BMC Bioinformatics* **7**, S7 (2006).
85. P. Langfelder, S. Horvath, WGCNA: An R package for weighted correlation network analysis. *BMC Bioinformatics* **9**, 559 (2008).
86. L. He, J. Davila-Velderrain, T. S. Sumida, D. A. Hafler, M. Kellis, A. M. Kulminski, NEBULA is a fast negative binomial mixed model for differential or co-expression analysis of large-scale multi-subject single-cell data. *Commun. Biol.* **4**, 629 (2021).
87. V. Kleshchevnikov, A. Shmatko, E. Dann, A. Aivazidis, H. W. King, T. Li, R. Elmentaite, A. Lomakin, V. Kedlian, A. Gayoso, M. S. Jain, J. S. Park, L. Ramona, E. Tuck, A. Arutyunyan, R. Vento-Tormo, M. Gerstung, L. James, O. Stegle, O. A. Bayraktar, Cell2location maps fine-grained cell types in spatial transcriptomics. *Nat. Biotechnol.* **40**, 661–671 (2022).
88. T. G. Beach, C. H. Adler, L. I. Sue, G. Serrano, H. A. Shill, D. G. Walker, L. Lue, A. E. Roher, B. N. Dugger, C. Maarouf, A. C. Birdsill, A. Intorcia, M. Saxon-Labelle, J. Pullen, A. Scroggins, J. Filon, S. Scott, B. Hoffman, A. Garcia, J. N. Caviness, J. G. Hentz, E. Driver-Dunckley, S. A. Jacobson, K. J. Davis, C. M. Belden, K. E. Long, M. Malek-Ahmadi, J. J. Powell, L. D. Gale, L. R. Nicholson, R. J. Caselli, B. K. Woodruff, S. Z. Rapscak, G. L. Ahern, J. Shi, A. D. Burke, E. M. Reiman, M. N. Sabbagh, Arizona study of aging and neurodegenerative disorders and brain and body donation program. *Neuropathology* **35**, 354–389 (2015).

89. H. Duong, M. Han, A multispectral LED array for the reduction of background autofluorescence in brain tissue. *J. Neurosci. Methods* **220**, 46–54 (2013).
90. N. Sweeney, T. Y. Kim, C. T. Morrison, L. Li, D. Acosta, J. Liang, N. V. Datla, J. A. Fitzgerald, H. Huang, X. Liu, G. H. Tan, M. Wu, K. Karelina, C. E. Bray, Z. M. Weil, D. W. Scharre, G. E. Serrano, T. Saito, T. C. Saido, T. G. Beach, O. N. Kokiko-Cochran, J. P. Godbout, G. V. W. Johnson, H. Fu, Neuronal BAG3 attenuates tau hyperphosphorylation, synaptic dysfunction, and cognitive deficits induced by traumatic brain injury via the regulation of autophagy-lysosome pathway. *Acta Neuropathol.* **148**, 52 (2024).
91. H. Fu, A. Possenti, R. Freer, Y. Nakano, N. C. Hernandez Villegas, M. Tang, P. V. M. Cauhy, B. A. Lassus, S. Chen, S. L. Fowler, H. Y. Figueroa, E. D. Huey, G. V. W. Johnson, M. Vendruscolo, K. E. Duff, A tau homeostasis signature is linked with the cellular and regional vulnerability of excitatory neurons to tau pathology. *Nat. Neurosci.* **22**, 47–56 (2019).
92. J.-R. Lin, B. Izar, S. Wang, C. Yapp, S. Mei, P. M. Shah, S. Santagata, P. K. Sorger, Highly multiplexed immunofluorescence imaging of human tissues and tumors using t-CyCIF and conventional optical microscopes. *Elife* **7**, e31657 (2018).
93. A. Patel, A. Garcia Diaz, J. C. Moore, D. Sirabella, B. Corneo, Establishment and characterization of two iPSC lines derived from healthy controls. *Stem Cell Res.* **47**, 101926 (2020).
94. W. B. Stine, K. N. Dahlgren, G. A. Krafft, M. J. LaDu, In vitro characterization of conditions for amyloid-beta peptide oligomerization and fibrillogenesis. *J. Biol. Chem.* **278**, 11612–11622 (2003).
95. D. Kim, J. M. Paggi, C. Park, C. Bennett, S. L. Salzberg, Graph-based genome alignment and genotyping with HISAT2 and HISAT-genotype. *Nat. Biotechnol.* **37**, 907–915 (2019).
96. M. I. Love, W. Huber, S. Anders, Moderated estimation of fold change and dispersion for RNA-seq data with DESeq2. *Genome Biol.* **15**, 550 (2014).
97. Y. Benjamini, Y. Hochberg, Controlling the false discovery rate: A practical and powerful approach to multiple testing. *J. R. Stat. Soc. B. Methodol.* **57**, 289–300 (1995).
98. S. H. Choi, Y. H. Kim, M. Hebisch, C. Sliwinski, S. Lee, C. D'Avanzo, H. Chen, B. Hooli, C. Asselin, J. Muffat, J. B. Klee, C. Zhang, B. J. Wainger, M. Peitz, D. M. Kovacs, C. J. Woolf, S. L. Wagner, R. E. Tanzi, D. Y. Kim, A three-dimensional human neural cell culture model of Alzheimer's disease. *Nature* **515**, 274–278 (2014).
99. Y. H. Kim, S. H. Choi, C. D'Avanzo, M. Hebisch, C. Sliwinski, E. Bylykbashi, K. J. Washicosky, J. B. Klee, O. Brüstle, R. E. Tanzi, D. Y. Kim, A 3D human neural cell culture system for modeling Alzheimer's disease. *Nat. Protoc.* **10**, 985–1006 (2015).
100. E. Kim, H. Kim, M. P. Jedrychowski, G. Bakiasi, J. Park, J. Kruskop, Y. Choi, S. S. Kwak, L. Quinti, D. Y. Kim, C. D. Wrann, B. M. Spiegelman, R. E. Tanzi, S. H. Choi, Irisin reduces amyloid-β by inducing the release of neprilysin from astrocytes following downregulation of ERK-STAT3 signaling. *Neuron* **111**, 3619–3633.e8 (2023).
101. M. Jorfi, J. Park, C. K. Hall, C.-C. J. Lin, M. Chen, D. Von Maydell, J. M. Kruskop, B. Kang, Y. Choi, D. Prokopenko, D. Irimia, D. Y. Kim, R. E. Tanzi, Infiltrating CD8+ T cells exacerbate Alzheimer's disease pathology in a 3D human neuroimmune axis model. *Nat. Neurosci.* **26**, 1489–1504 (2023).
102. E. M. Abud, R. N. Ramirez, E. S. Martinez, L. M. Healy, C. H. H. Nguyen, S. A. Newman, A. V. Yeromin, V. M. Scarfone, S. E. Marsh, C. Fimbres, C. A. Caraway, G. M. Fote, A. M. Madany, A. Agrawal, R. Kayed, K. H. Gylys, M. D. Cahalan, B. J. Cummings, J. P. Antel, A. Mortazavi, M. J. Carson, W. W. Poon, M. Blurton-Jones, iPSC-derived human microglia-like cells to study neurological diseases. *Neuron* **94**, 278–293.e9 (2017).
103. J. Hasselmann, M. A. Coburn, W. England, D. X. Figueroa Velez, S. Kiani Shabestari, C. H. Tu, A. McQuade, M. Kolahdouzan, K. Echeverria, C. Claes, T. Nakayama, R. Azevedo, N. G. Coufal, C. Z. Han, B. J. Cummings, H. Davtyan, C. K. Glass, L. M. Healy, S. P. Gandhi, R. C. Spitale, M. Blurton-Jones, Development of a chimeric model to study and manipulate human microglia in vivo. *Neuron* **103**, 1016–1033.e10 (2019).

Acknowledgments: This manuscript has been reviewed by DIAN Study investigators for scientific content and consistency of data interpretation with previous DIAN Study publications. We acknowledge the altruism of the participants and their families and the contributions of the DIAN research and support staff at each participating site for contributions to this study. We are grateful to the Banner Sun Health Research Institute Brain and Body Donation Program of Sun City, Arizona for the provision of human biological materials. The data available in the AD Knowledge Portal would not be possible without the participation of research volunteers and the contribution of data by collaborating researchers. The results published here are in whole or in part based on data obtained from the AD Knowledge Portal (https://adknowledgeportal.org). This work was supported by access to equipment made possible by the Hope Center for Neurological Disorders and the Departments of Neurology and Psychiatry at Washington University School of Medicine. We thank B. Corneo for advice on iPSC protocols and W. Wang and C. (L.) Lu for assisting with fluorescence-activated cell sorting. Novogene conducted iMGL cell sequencing and preliminary RNA-seq data processing. Support for title page creation and format was provided by AuthorArranger, a tool developed at the National Cancer Institute. For the acknowledgments of Alzheimer's Disease Neuroimaging Initiative (ADNI), data used in preparation of this article were obtained from the ADNI database (adni.loni.usc.edu). Hence, the investigators within the ADNI contributed to the design and implementation of ADNI and/or provided data but did not participate in analysis or writing of this report. A complete listing of ADNI investigators can be found at http://adni.loni.usc.edu/wp-content/uploads/how_to_apply/ADNI_Acknowledgement_List.pdf. ADNI is funded by the National Institute on Aging, the National Institute of Biomedical Imaging and Bioengineering and through contributions from the following: AbbVie, Alzheimer's Association, Alzheimer's Drug Discovery Foundation, Araclon Biotech, BioClinica Inc., Biogen, Bristol-Myers Squibb Company, CereSpir Inc., Cogstate, Eisai Inc., Elan Pharmaceuticals Inc., Eli Lilly and Company, EuroImmun, F. Hoffmann–La Roche Ltd. and its affiliated company Genentech Inc., Fujirebio, GE Healthcare, IXICO Ltd., Janssen Alzheimer Immunotherapy Research & Development LLC., Johnson & Johnson Pharmaceutical Research & Development LLC., Lumosity, Lundbeck, Merck & Co. Inc., Meso Scale Diagnostics LLC., NeuroRx Research, Neurotrack Technologies, Novartis Pharmaceuticals Corporation, Pfizer Inc., Piramal Imaging, Servier, Takeda Pharmaceutical Company, and Transition Therapeutics. The Canadian Institutes of Health Research is providing funds to support ADNI clinical sites in Canada. Private sector contributions were facilitated by the Foundation for the National Institutes of Health (www.fnih.org). The grantee organization is the Northern California Institute for Research and Education, and the study is coordinated by the Alzheimer's Therapeutic Research Institute at the University of Southern California. ADNI data are disseminated by the Laboratory for Neuro Imaging at the University of Southern California. **Funding:** This research was supported by National Institute on Aging grants U01AG072464 (to O.H. and C.M.K.), R56AG067764 (to O.H.), R01AG067606 (to T.-W.K.), R01AG062734 (to C.M.K.), R01AG075092 (to H.F.), P30AG066444 (to J.C.M.), P01AGO26276 (to J.C.M.), P01AG003991 (to J.C.M.), and K99AG086583 (to R.D.A.); National Institute of Neurological Disorders and Stroke grants R21NS127211 and R01NS118146 (to B.A.B.); Department of Defense grant W81XWH1910309 (to H.F.), and Chan Zuckerberg Initiative (to O.H. and C.M.K.). This is also supported by National Institute on Aging grant U19AG032438 (DIAN), Alzheimer's Association grant SG-20-690363-DIAN (DIAN); German Center for Neurodegenerative Diseases (DIAN); Raul Carrea Institute for Neurological Research (DIAN); Japan Agency for Medical Research and Development (DIAN); Korea Health Industry Development Institute (DIAN); Spanish Institute of Health Carlos III (DIAN); Canadian Institutes of Health Research (DIAN); Canadian Consortium of Neurodegeneration and Aging (DIAN); Brain Canada Foundation (DIAN); Fonds de Recherche du Québec–Santé (DIAN); National Institute of Neurological Disorders and Stroke grant U24 NS072026 (BDPSC); National Institute on Aging grants P30 AG019610 and P30AG072980 (BDPSC); Arizona Department of Health Services contract 211002 (BDPSC); Arizona Biomedical Research Commission contracts 4001, 0011, 05-901, and 1001 (BDPSC); Michael J. Fox Foundation for Parkinson's Research (BDPSC); and the Gates Sr. Alzheimer's Disease Research Fellowship from the Alzheimer's Disease Data Initiative (RDA). **Author contributions:** O.H., T.-W.K., R.D.A., and G.M.F. conceptualized the study. O.H., T.-W.K., R.D.A., G.M.F., H.F., R.E.T., and D.Y.K. designed the study. J.C.M., D.M.H., E.M., M.F., J.P.C., and G.T.S. performed the donor recruitment, tissue procurement, and clinical characterization. R.J.P. performed the neuropathology. L.B., S.-F.Y., and B.C.N. performed the human single-cell processing, cleaning, and analyses. R.D.A. analyzed the snRNA-seq and bulk RNA-seq data for all CellPhoneDB, CytoTalk, and iMGL analyses. G.M.F. performed the CRISPR-Cas9 KO, generated the iMGL, and performed the in vitro experiments. E.M.M. consulted on phagocytosis experiments. D.Y.K., Y.R., and J.P. performed the triculture experiments. Q.G. and Q.M. performed the spatial transcriptomics quality control and analyses. N.S., T.Y.K., and S.C. performed the quantitative cyclic multiplex immunofluorescence. O.H., T.-W.K., R.D.A., G.M.F., H.F., A.K., M.A., P.M.R.P., B.A.B., L.P., and C.M.K. interpreted the results. The manuscript was written and edited by O.H., T.-W.K., R.D.A., G.M.F., H.F., C.M.K., B.A.B., A.K., and M.A., with input from all authors. **Competing interests:** T.-W.K. is a cofounder of BL Melanis Co. Ltd. D.M.H. cofounded and is on the scientific advisory board of C2N Diagnostics. D.M.H. consults for Genentech, Denali, Cajal Neurosciences, and Alector. J.C.M. is a consultant for the Barcelona Brain Research Center (BBRC) and the TS Srinivasan Advisory Board. J.C.M. is a consultant for the Barcelona Brain Research Center (BBRC) and the TS Srinivasan Advisory Board. J.C.M. is an advisory board member for the Cure Alzheimer's Fund Research Strategy Council. J.C.M. receives research support from the NIH and the Alzheimer's Association (US) and is a member of the advisory board for Humana Healthcare. E.M. receives research support from the NIA, Hoffman-LaRoche, and Eli Lilly; is a member of advisory boards for Eli Lilly, Alector, and the NIA; and holds a leadership role in Foundation Alzheimer and Alzamend. All other authors declare that they have competing interests. **Data and materials availability:** All data associated with this study are present in the paper or the Supplementary Materials. Human iMGL bulk RNA-seq data are available under GEO accession GSE226507. The snRNA-seq data from the Knight ADRC are publicly available by request from the National Institute on Aging Genetics of Alzheimer's Disease Data Storage Site (NIAGADS) under accession number NG00108 (www.niagads.org/datasets/ng00108). DIAN brain bank snRNA-seq data access requires a request through https://dian.wustl.edu/our-research/for-investigators. All scripts necessary to reproduce the figures from this manuscript are available at Zenodo (https://doi.org/10.5281/zenodo.15763232).

Submitted 25 February 2025
Accepted 20 May 2025
Published 30 July 2025
10.1126/scitranslmed.adx0027